# PLASMA DIAGNOSIS BY MEANS OF PHOTON-ELECTRON SCATTERING

Thesis by

Steven Emanuel Schwarz

In Partial Fulfillment of the Requirements
For the Degree of
Doctor of Philosophy

California Institute of Technology
Pasadena, California
1964
(Submitted May 20, 1964)

## ACKNOWLEDGEMENTS

The author wishes to thank his thesis advisor, Professor Nicholas George, for his most helpful guidance throughout the conduct of the work. He further wishes to thank Dr. R. W. Gould for his initial suggestion of the problem, and Dr. F. J. McClung for his invaluable advice on laser techniques.

He further wishes to thank Dr. G. F. Smith, Dr. Harvey Winston, Dr. R. W. Hellwarth, and the many others of his friends and associates who have taken a kind interest in the project. The assistance of Mr. Ernest Lampron, Mr. Matthew Himber, and Mr. Robert Hallden during construction of the equipment, and of Mrs. Olive List during preparation of the manuscript, is gratefully acknowledged.

The author has received generous financial support under a Howard Hughes Doctoral Fellowship. Additional support has been received from research funds of the United States Air Force and The National Aeronautics and Space Administration.

## ABSTRACT

When a pulse of intense light from a giant-pulse laser passes through a plasma, a very small fraction of the light is scattered out of the beam as a result of ("Thomson") scattering by free electrons. Under suitable conditions the intensity of the scattered light is proportional to the density of free electrons, while its spectral distribution is related to the velocity distribution of the free electrons through the Doppler formula.

Theoretical considerations, relating to the conditions of validity of the method, are discussed. Various mechanisms which could interfere with the diagnostic technique are mentioned and their importance considered. Design considerations for diagnostic experiments are then taken up, and signal-to-noise ratios calculated.

An apparatus for conducting scattering experiments has been constructed. Phenomenological checks indicate that the observed scattering is by free electrons. Measurements conducted at various times in the development of an afterglow plasma indicate Doppler broadening of the scattered light; the broadening disappears as the electrons cool during the first three microseconds of the afterglow. Measurements of electron density as a function of time are made in the afterglow, and are calibrated by means of Rayleigh scattering from gas at a known pressure.

Two unexpected laser-plasma interactions have been observed. The first is designated as "induced plasma luminosity" and the second

as "giant scattering." Both effects appear to be related to the presence of hydrocarbon impurities in the gas.

# TABLE OF CONTENTS

# CHAPTER I

# INTRODUCTION

## A. Historical Background

The scattering of electromagnetic waves by free electrons, often called Thomson scattering, is a well-known phenomenon of physics. In stellar atmospheres it plays a role in the transfer of energy; in the terrestrial ionosphere it can be used to provide high frequency radio communication. Yet while familiar on a large scale, Thomson scattering has been something of a stranger to the laboratory, because the cross-section for the process is inconveniently small.

In the x-ray region, scattering by electrons has been known for several decades, and the spectral density of Compton scattering has been used as a device to study the distribution of velocities of atomic electrons and conduction electrons in solids.[I-1] Interest in the effect at lower frequencies was stimulated, more recently, by ionospheric radio back-scatter experiments proposed by Gordon [I-2] and carried out by Bowles.[I-2] [I-3] Among the results of these experiments was the surprising observation that the spectral distribution of the scattered radiation was not Doppler-broadened to a degree consonant with the known electron velocities of the ionosphere. This led to the development of theories of scattering from plasma by Fejer, [I-5] [I-6] Dougherty and Farley, [I-7] [I-8] Salpeter, [I-9] and others; at present these theories seem adequate to explain experimental observations.

New possibilities for laboratory investigation of Thomson

scattering have appeared in the last few years, arising from the development of the optical maser. Thomson scattering of radiation in the optical region has now become a subject of considerable interest, both for the sake of experimental verification of the theory, and for its possible applications, one of which is the subject of this thesis.

## B. Nature of the Problem

On many occasions the experimental plasma physicist will wish to diagnose the electron density and electron velocity distribution within a given plasma. In general neither measurement is easily made. Of the common diagnostic methods, microwave interferometry is difficult above certain densities, and provides a density measurement which is an average over an inconveniently large volume whose dimensions are of the order of a wavelength. Probe measurements, on the other hand, suffer under numerous interpretive difficulties, may disturb the plasma, and are difficult to perform so as to provide time resolution. Measurements by means of Stark broadening of spectral lines are useful only above certain densities, (their minimum lying above the maximum density for microwave work); moreover, theoretical profiles for comparison are available only for simple atomic structures, and even then are somewhat doubtful. New diagnostic techniques, therefore, are badly needed.

It has been pointed out by many persons that Thomson scattering of laser light could serve as a new diagnostic method. In concept the idea is similar to radar: one sends out a pulse of light, and receives the light scattered out of the beam by the electrons; the

intensity of the scattering indicates the number of scatterers, while the Doppler shifts of the scattered light indicates their velocity distribution. By this means one may hope to perform measurements within an infinitesimal volume having dimensions approaching the wavelength of light, and without disturbing the plasma whose properties are being measured; this could be done even in the case of many plasmas whose characteristics of geometry or ionization density make them unamenable to conventional diagnostic methods. However, although the idea is simple in theory it is difficult to carry out in practice. For plasmas of moderate density, such a very small portion of the incident light is scattered out of the beam that extensive precautions must be taken, so that the desired signal will not be masked by spurious reflections from the walls of the apparatus. Moreover, even with the highly intense laser light source, the magnitude of the signal is small enough to pose problems in its detection.

At the time that this work was begun, Thomson scattering of light in the laboratory had never been observed. Since the work has been in progress, four experiments on the subject have been reported. Fiocco and Thompson [I-10] have achieved the first observation of optical Thomson scattering. This was done using a 20-joule normal ruby laser and an electron beam of $5 \cdot 10^9/cm^3$ density. The same workers have also reported scattering from the plasma of a hollow-cathode discharge.[I-11] The latter observations have since been modified by the detection of the presence of photoionization processes, which result in additional luminosity that appears in addition to the true plasma

scattering.[I-12] Scattering from a Theta-pinch plasma has been reported by Fuenfer, Kronast and Kunze.[I-13] A preliminary report of the present work, which includes one of the earliest observations of thermal broadening and the first application of the giant-pulse laser technique, has also been published.[I-14]

In this thesis we begin in Chapter II with a review of the theory of scattering from plasmas. Included in the discussion are considerations of the limits of validity of plasma diagnostic experiments, set by collective plasma scattering behavior, absorption of energy by the plasma, and high-field effects. Scattering from neutral atoms and positive ions is also discussed, and the relevance of the former for purposes of calibration is pointed out. In Chapter III we consider the general experimental problem of detection of optical Thomson scattering in the laboratory, with specific attention to the use of the giant-pulse laser as a light source. Noise considerations for such experiments are derived, and applications of the noise theory are pointed out. The apparatus which has been constructed here is then described, and various suggestions for the improvement of the method in future experiments are presented.

Chapter IV reports the exploratory experiments which have been carried out. One novel feature of the apparatus is its use of the giant-pulse laser as light source. In addition to the advantages of the scattering method previously mentioned, the giant-pulse technique represents an improvement over previous work in that it allows measurements to be made "instantaneously", and hence is suitable for the study

of plasmas which vary in time. A further advantage of the giant-pulse technique, to be seen from the calculations of Chapter III, is that under conditions of interference from plasma self-luminosity, the giant-pulse technique provides an improved signal-to-noise ratio over that obtained when a normal laser of similar energy is used. The apparatus to be described also is the first to be constructed in which spurious reflections from the walls do not interfere with the measurements. In other work the light scattered from the plasma has been distinguished from that scattered from the walls only by means of spectral separation of the former through Doppler broadening; in the present work so little wall scattering remained that separation of the signal by Doppler broadening was not necessary, and hence "cold" plasmas could for the first time be treated.

## REFERENCES


I-1. J. W. M. DuMond, Rev. Mod. Physics 5 1-33 (1933).

I-2. W. E. Gordon, Proc. I.R.E. 46, 1824-25 (1958).

I-3. K. L. Bowles, Phys. Rev. Letters 1, 454-57 (1958).

I-4. K. L. Bowles, J. Research of National Bureau of Standards, 65 D, 1-14 (Sept. 1, 1960).

I-5. J. A. Fejer, Canadian J. Physics 38, 1114-33 (1960).

I-6. J. A. Fejer, Canadian J. Physics 39, 716-40 (1961).

I-7. J. P. Dougherty and D. T. Farley, Proc. Roy. Soc. A259, 79-99 (1960).

I-8. J. P. Dougherty and D. T. Farley, Proc. Roy. Soc. A263, 238-58 (1961).

I-9. E. E. Salpeter, Phys. Rev. 120, 1528-35 (Dec. 1, 1960).

I-10. G. Fiocco and E. Thompson, Phys. Rev. Letters 10, 89-91 (Feb. 1, 1963).

I-11. G. Fiocco and E. Thompson, Bulletin of Am. Phys. Soc., 8, 372 (April, 1963).

I-12. D. J. Rose, L. M. Lidsky, E. Thompson, 5th Annual Meeting of A.P.S. Division of Plasma Physics, San Diego, Calif., (Nov. 1963); also E. Thompson, private communication.

I-13. E. Fuenfer, B. Kronast and H-J. Kunze, Physics Letters 5, 125-7 (June, 1963).

I-14. S. E. Schwarz, Proc. I.E.E.E. 51, 1362 (Oct. 1963).

# CHAPTER II

# SCATTERING THEORY

## A. Incoherent Free-Electron Scattering

A familiar result of classical electromagnetic theory is the phenomenon of Thomson scattering of radiation by free electrons.[II-1] Let us consider the scattering by a single free electron of a monochromatic, plane, linearly polarized wave whose electric vector at $\underset{\sim}{r}$, the location of the particle, and in the particle's rest system, may be written,

$$\underset{\sim}{E} = \underset{\sim}{E}_o \cos (\underset{\sim}{K} \cdot \underset{\sim}{r} + \omega t + \alpha) \qquad \text{(II-1)}$$

where $\underset{\sim}{E}_o$ is a constant vector, $\underset{\sim}{K}$ is the propagation vector, $\omega$ the frequency, $t$ the time, and $\alpha$ an arbitrary phase constant. We assume that the velocities acquired by the electron in the field are always much smaller than the speed of light $c$, so that the influence of the magnetic field on the particle may be neglected. In this case the motion of the electron is transverse to the direction of wave propagation, so that the equation of motion of the charge in its rest system is

$$m\ddot{\underset{\sim}{r}} = e\underset{\sim}{E}_o \cos (\omega t - \beta) \qquad \text{(II-2)}$$

where $\beta$ is another arbitrary phase constant. Since the charged particle undergoes acceleration, re-radiation takes place. Let us employ the familiar formula for the differential power $dI$ radiated

in the direction $\underline{n}$ by an accelerated point charge into differential solid angle $d\Omega$ [II-2]:

$$dI = \frac{e^2}{16\pi^2\epsilon_o c^3} (\ddot{\underline{r}} \times \underline{n})^2 \, d\Omega \qquad \text{(II-3)}$$

The "differential scattering cross-section" $d\sigma$ is defined to be the quotient of the time-average power radiated into $d\Omega$ by the time-average incident power per unit area. The latter is the time-average Poynting vector, equal to $\frac{1}{2}\sqrt{\frac{\epsilon_o}{\mu_o}} \left|E_o\right|^2$. Taking the time-average of $dI$ and dividing

$$d\sigma = \left(\frac{e^2}{4\pi\epsilon_o mc^2}\right)^2 \sin^2 \psi \, d\Omega \qquad \text{(II-4)}$$

where $d\sigma$ is the differential scattering cross-section and $\psi$ is the angle between the scattering direction and the electric vector of the incident wave. The total cross-section $\sigma_o$, equal to the integral of $d\sigma$ over all directions, is then

$$\sigma_o = \frac{8\pi}{3}\left(\frac{e^2}{4\pi\epsilon_o mc^2}\right)^2 = \frac{8}{3}(\pi r_o^2) \qquad \text{(II-5)}$$

where $r_o$ is the quantity usually known as the "classical radius of the electron". $\sigma_o$, called the Thomson cross-section, has the value $6.6 \cdot 10^{-25}$ cm$^2$. This classical result is in agreement with quantum-mechanical calculations, provided that the photon energy is much less than the rest energy $mc^2$ of the electron. Above such energy the Klein-Nishina formula must be used. One finds from it that the differential

scattering cross-section in the forward direction retains its classical value but the scattering in all other directions is decreased. Hence the scattering becomes peaked in the forward direction and the total cross-section is decreased.

Let us now consider an ensemble of such electron scatterers. We shall first assume that there is no interaction whatsoever between one particle and another; their positions and velocities are not correlated in any way. When such an ensemble is observed from any direction except the forward direction, the phase difference between the waves emerging from any two of the scatters will be a random quantity, taking any value from zero to $2\pi$ with equal probability. Such scattering is called incoherent scattering, and has the property that the intensity of scattered radiation will be proportional to the first power of the number of scatterers.* If in addition the scatterers are in motion, monochromatic light which is scattered by them will exhibit broadening according to the familiar Doppler formula. The problem of finding the spectral distribution of incoherently scattered radiation has been treated in the "slightly relativistic" approximation (terms of

---

* If the region of scattering is limited in size to dimensions on the order of a wavelength, it is possible that "partial coherence" effects may still occur. Let the approximate dimension of the scattering region be a. Then for scattering angles less than $c/\omega a$ partially coherent scattering will be in evidence, characteristically leading to an increase in scattered intensity in such directions. (A familiar example occurs in the scattering of x-rays by the cluster of electrons contained in an atom.) Partial coherence effects might conceivably arise in the experiments to be described if it should happen that the ionization is localized in small regions or if the laser light were only coherent over small areas. However there is no *a priori* reason to expect that such effects are present.

order $v/c$ retained) by Papas and Lee.[II-3] Let $f(\beta_x,\beta_y,\beta_z)$ be the velocity distribution function of the scatterers (where $\beta_x = v_x/c$, etc.), such that $\iiint_{-\infty}^{\infty} f(\beta_x,\beta_y,\beta_z)\, d\beta_x\, d\beta_y\, d\beta_z = n$, the number of scatterers per unit volume. Then the results of Papas and Lee give

$$W(\theta,\varphi,\omega)\, d\Omega\, d\omega = \frac{d\Omega d\omega}{\omega_o(1-\cos\theta)} \iint_{-\infty}^{\infty} W_o(\theta,\varphi)\, f\left(\beta_x,\beta_y,\frac{\omega_o-\omega}{\omega_o(1-\cos\theta)} + \frac{\beta_y \sin\theta}{1-\cos\theta}\right) d\beta_x\, d\beta_y \qquad \text{(II-6)}$$

where $W_o(\theta,\varphi,\omega)\, d\omega\, d\Omega$ is the power scattered into the solid angle $d\Omega$ and frequency range $(\omega,\omega+d\omega)$ per unit scattering volume, $\theta$ is the angle between the incident wave and scattered wave directions, $\varphi$ the angle between the incident wave electric vector and the scattering plane, $\omega_o$ the incident wave angular frequency, and $W(\theta,\varphi)d\Omega$ the power scattered into solid angle $d\Omega$ by a single electron, which is found to be

$$\begin{aligned} W_o\, d\Omega = {} & \frac{c}{4\pi} E_o^2\, r_o^2\, (1 - \sin^2\theta\cos^2\varphi)\, d\Omega \\ & + \frac{c}{4\pi} E_o^2\, r_o^2 \Big[\beta_x \sin 2\varphi \sin\theta(\cos\theta - 1) + 2\beta_y \sin\theta\,(3 - 3\sin^2\theta\cos^2\varphi \\ & - \sin^2\varphi - \cos\theta\cos^2\varphi) + 2\left\{\frac{\omega_o-\omega}{\omega_o(1-\cos\theta)} + \frac{\beta_y\sin\theta}{1-\cos\theta}\right\} \times \\ & \times \{(3\cos\theta - 1)(1 - \sin^2\theta\cos^2\varphi) - \cos\theta\}\Big]\, d\Omega \qquad \text{(II-7)} \end{aligned}$$

If $v/c \ll 1$ and if we are not dealing with the vicinity of $\theta = \frac{\pi}{2}$, $\varphi = 0$,

only the first term of Eq. II-7 (zero order in v/c) need be retained. This leaves

$$W(\theta,\varphi,\omega)\, d\Omega\, d\omega = \frac{cE_o^2 r_o^2 (1 - \sin^2\theta \cos^2\varphi)}{4\pi\omega_o (1 - \cos\theta)} d\Omega\, d\omega \times$$

$$\times \int\int_{-\infty}^{\infty} f\left(\beta_x, \beta_y, \frac{\omega_o - \omega}{\omega_o (1 - \cos\theta)} + \frac{\beta_y \sin\theta}{1 - \cos\theta}\right) d\beta_x\, d\beta_y \qquad \text{(II-8)}$$

In some circumstances it is possible to assume that the velocity distribution of the scatterers is Maxwellian, in which case the electrons velocity distribution is defined simply by a temperature T. In this case the result of Papas and Lee for non-relativistic particle velocities is

$$W(\theta,\varphi,\omega)\, d\Omega\, d\omega = \frac{nc^2 r_o^2 E_o^2}{8\pi\omega_o} \frac{m^{\frac{1}{2}}}{\pi\kappa T} \frac{1 - \sin^2\theta \cos^2\varphi}{1 - \cos\theta} \times$$

$$\times \exp\left[-\frac{mc^2 (\omega_o - \omega)^2}{2\omega_o^2 \kappa T (1 - \cos\theta)}\right] d\Omega\, d\omega \qquad \text{(II-9)}$$

where m is the electron mass and $\kappa$ is the Boltzmann constant.

Equations II-8 and II-9 are the basis of the method of plasma diagnosis under consideration in this thesis. We apply the incident wave (Eq. II-1), and detect the energy scattered from the plasma. In the general case of arbitrary particle velocities the scattered intensity and spectral distribution will be related to the electron density and velocity distribution according to Eq. II-8, and in the special case of thermal equilibrium, according to II-9. One then "works

backwards" by means of these formulas to gain information about the internal condition of the plasma. The remainder of this chapter will be concerned with the limits of validity of Eqs. II-8 and II-9, with respect to such possibly disruptive mechanisms as collective plasma effects and perturbation of the state of the plasma by the incident wave.

## B. Collective Plasma Scattering Effects

In the previous section we have considered the scattering of radiation by electrons which are assumed not to interact with one another. That this is an idealization is evident, since in a physical plasma every electron does indeed interact with every other, through the coulomb force. To determine the limits of validity of the incoherent scattering theory it is necessary to consider the collective plasma effects. An important result of such calculations, which are summarized below, is that collective effects do not modify the incoherent scattering theory significantly when

$$\frac{4\pi\lambda_D}{\lambda} \sin\frac{\theta}{2} \gg 1 \qquad \text{(II-10)}$$

Here $\lambda$ is the incident wavelength and $\lambda_D$ is the Debye length, equal to $(\kappa T/4\pi ne^2)^{\frac{1}{2}}$.

The scattering of radiation from plasmas has been considered by numerous workers, including Buneman, [II-4] Dougherty and Farley, [II-5] Fejer, [II-6] and Salpeter.[II-7] The point of view taken by all these workers is that the scattering is from sinusoidal fluctuations in the electron density. Let $k = 4\pi\lambda^{-1} \sin(\theta/2)$. Then it is

evident that the amplitude of the scattered radiation is proportional to the quantity $\rho_{ke}$, defined as

$$\rho_{ke} = -e \sum_{j=1}^{n} e^{-i\underline{k} \cdot \underline{r}_j} \qquad \text{(II-11)}$$

where $\underline{r}_j$ is the position of the jth electron, and $\underline{k}$ is a vector of magnitude $k$ in the scattering plane bisecting the external angle between the incident and scattering directions. (The orientation of $\underline{k}$ is actually irrelevant since the plasma is being assumed isotropic.) The intensity of the returned light is therefore proportional to $< \rho_{ke}^* \rho_{ke} >$ (where $<>$ denotes expectation value). The scattered energy in the frequency interval $(\omega_o, \omega_o + d\omega)$ (where $\omega_o$ is the incident frequency) is proportional to $< \left| Q_e(\omega) \right|^2 >$, where $Q_e$ is the temporal fourier transform of $\rho_{ke}$,

$$Q_e(\omega) = \int_0^\infty dt \; \rho_{ke}(t) \; e^{-\gamma t} \; e^{-i\omega t} \qquad \text{(II-12)}$$

(The finite duration of the measurement is included in the quantity $Q_e(\omega)$. The point of view taken is that the density fluctuations are "turned on" at $t = 0$, and decay as $e^{-\gamma t}$, corresponding to a measurement of duration $\approx (2\gamma)^{-1}$. Since eventually a time average is taken with the duration approaching infinity, the manner of "turn-on" and "turn-off" are unimportant.) The problem is then reduced to finding the temporal and spatial transforms of the electron concentration under the influence of the plasma fields. The following results are those of Salpeter.

It is assumed that $n\lambda_D^3 \gg 1$, which insures that coulomb interaction energies are small compared with thermal energies, so that a treatment based on an equilibrium Maxwellian distribution of velocities is possible. Mean free paths are longer than $k^{-1}$ and $\lambda_D$. An important parameter $\alpha$ is defined:

$$\alpha = (k\lambda_D)^{-1} = \lambda(ne^2/4\pi\kappa T)^{\frac{1}{2}} (\sin \tfrac{1}{2}\theta)^{-1} \qquad \text{(II-13)}$$

Then it is found that

$$< \rho_{ke}^* \rho_{ke} > = ne^2 (1 + Z\alpha^2) \left[1 + (Z+1)\alpha^2\right]^{-1} \qquad \text{(II-14)}$$

where $Ze$ is the charge on each ion. The limit $\alpha \to o$ corresponds to the case of Eq. II-10, and the incoherent scattering theory obtains. As $\alpha$ is increased the total scattered power decreases and in the limit $\alpha \to \infty$ it is reduced by the factor $Z/(Z+1)$. The result obtained for the spectrum of the scattered light is

$$\frac{r}{\pi^{\frac{1}{2}} ne^2} < \left|Q_e(\omega)\right|^2 > d\omega = \Gamma_\alpha(x) \frac{d\omega}{\omega_e} + Z \left(\frac{\alpha^2}{1+\alpha^2}\right)^2 \Gamma_\beta(y) \frac{d\omega}{\omega_i} \qquad \text{(II-15)}$$

Here $\omega_e$ and $\omega_i$ are defined as

$$\omega_e = (2k^2\kappa T/m)^{\frac{1}{2}}$$

$$\omega_i = (2k^2\kappa T_i/M)^{\frac{1}{2}} \qquad \text{(II-16)}$$

where $M$ and $T_i$ are the ion mass and temperature; these quantities represent the Doppler frequencies that would be observed due to thermal velocities if incoherent scattering were taking place. The quantity $\beta$ is defined by

$$\beta^2 = \frac{ZT\alpha^2}{T_i\,(1+\alpha^2)} \tag{II-17}$$

$x = \omega/\omega_e$ and $y = \omega/\omega_i$, and the function $\Gamma$ is

$$\Gamma(x) = e^{-x^2}\left\{\left[1+\alpha^2 - 2\alpha^2 x\, e^{-x^2}\int_0^x e^{t^2}\,dt\right]^2 + \pi\alpha^4 x^2\, e^{-2x^2}\right\}^{-1} \tag{II-18}$$

When the function $\Gamma$ (Fig. II-1), which is applicable for the case $T_i = T$, $Z = 1$, and $m \ll M$, is studied, the following behavior is found. The integral over $d\omega$ decreases by one-half as $\alpha$ ranges from zero to infinity, as expected from Eq. II-14. For $\alpha \ll 1$ the function has the gaussian shape expected of incoherent scattering. For $\alpha = 1$ the maximum at $x = 0$ has become less pronounced, and for larger values the function near $x = 0$ is further diminished while a "spike" appears and grows higher in the vicinity of $(\omega - \omega_o)^2 \approx \omega_p^2 + 3\kappa Tk^2/m$, that is at Doppler shifts corresponding to the plasma frequency. Although the maximum of this peak becomes large with increasing $\alpha$, its width decreases, so that the area beneath it is of the order of $\alpha^{-2}$ times the area under the curve in the vicinity of the origin. In general the spectrum is composed of the contributions of both terms on the right side of Eq. II-15, which result respectively from electrons moving freely and from electrons whose motions are correlated with the ion

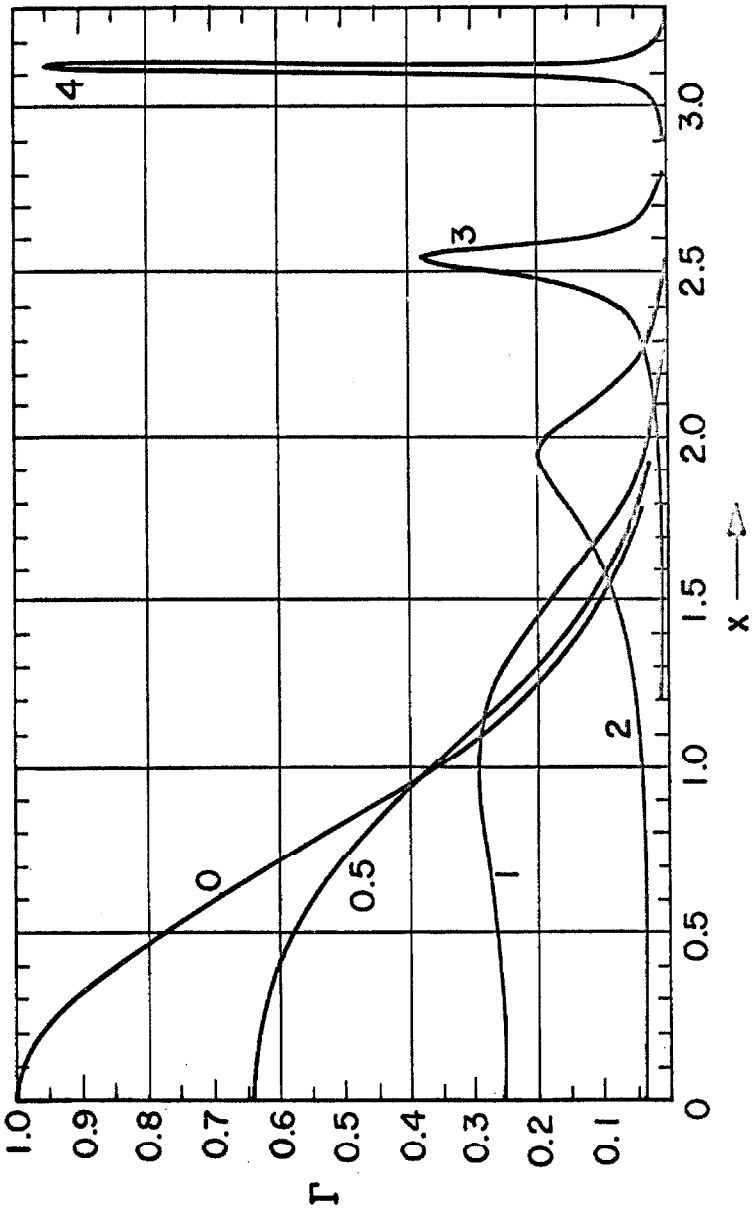


Figure II-1: The function Γ(x) of Eq. II-18, for alpha equal to 0, $\frac{1}{2}$, 1, 2, 3, and 4. (After Salpeter.)

motions. However if $\alpha \ll 1$ the first term is dominant, and in general the first term is adequate for values of $(\omega - \omega_o)$ large enough to be observed with present techniques.

The structure predicted by Eq. II-18 has been partially verified by microwave ionospheric backscatter measurements. It also lies within the range of possible optical experiments, provided that dense plasmas are employed, and such experiments will no doubt be performed soon. In the experiments discussed in this thesis, however, the quantity $\alpha$ is always less than one, and in most cases the incoherent scattering theory will apply. In cold afterglow measurements, where $\lambda_D$ is particularly small, correction by means of Eq. II-14 may be required.

## C. Disturbance of Plasma by Optical Fields

In all of the foregoing discussion it has been assumed that the state of the plasma being diagnosed is not altered by the optical fields applied. One may expect that for sufficiently high fields this will not be the case. Disturbance of the plasma is, of course, highly undesirable from the point of view of plasma diagnostics.

One may first inquire whether any new density fluctuations can be created in the plasma. This question has been answered in the negative by W. H. Kegel, [II-8] who showed that within the validity of the linearized Vlasov equation, no such fluctuations are produced, essentially because the electron motions are transverse. When a magnetic field is introduced the electrons experience $\underline{v} \times \underline{B}$ forces, and density fluctuations are produced. For the case of a homogeneous constant

magnetic field B oriented perpendicularly to the propagation direction and electric vector, the result is

$$\langle |n(k_o,\omega_o)|^2 \rangle = E^2 B^2 \frac{n_o^2}{\omega_o^4} \frac{e^4}{mc} \cdot 4 \frac{4\pi^2-6}{6} \qquad \text{(II-19)}$$

where $n(k_o,\omega_o)$ is the temporal and spatial fourier transform of the electron density, $n_o$ the equilibrium density, E the incident field, and $\omega_o$ the incident frequency. Without the magnetic field no density fluctuations are introduced.

Another possible sort of disturbance of the plasma would take place if its gross properties - density or temperature - were altered by the incident light. This question is susceptible to analysis for the case of a hydrogen plasma. One assumes thermodynamic equilibrium, and sums the probabilities for bound-free and free-free transitions, weighted by the appropriate level populations. The resulting absorption coefficient per atom in the ground state, is

$$\chi = \frac{64\pi^4}{3\sqrt{3}} \frac{me^{10}}{ch^3\kappa^3} \frac{e^{-u_1}}{T^3} \frac{1}{u^3} \left\{ \sum_{u_N<u}^{u_4} \frac{u_N}{N^3} + \frac{u_5}{2u_1} \right\} \qquad \text{(II-20)}$$

Here m and e are the electronic mass and charge, h the Planck constant, $u = h\nu/\kappa T$, $u_N = Rhc/N^2\kappa T$, and R is the Rydberg constant. [II-9] The terms of the sum inside the brackets refers to transitions from the lower photo-ionizable bound states to the continuum, and is to include only the values of N (principal quantum number) for which photoionization is possible. The sum of the transitions from the fifth

and higher levels is approximated as an integral and combined with the free-free transitions to compose the second term in the brackets. Using formula II-20 we can calculate the absorption of energy from a laser beam, which is $E = n_o \chi \tau I$, where $n_o$ is the number of atoms in the ground state, $I$ the intensity of the laser beam, and $\tau$ its duration. Let us take $T = 5$ eV, $I = 10^8$ watts/cm$^2$, $\tau = 10^{-7}$ second. We consider the cases of electron density = (1) $10^{14}$/cc and (2) $10^{17}$/cc. From the Saha equation we obtain the density of atoms in the ground state to be for case (1), $4.6 \cdot 10^6$/cm$^3$ and for case (2), $4.6 \cdot 10^{12}$/cm$^3$. For case (1) we find that the energy absorbed amounts to approximately $2 \cdot 10^{-4}$ eV per electron. The absorbed energy per electron increases roughly as the electron density, so that for case (2) we have absorption of 0.2 eV per electron. (If we had chosen a twenty-joule normal laser focused to 1 mm$^2$ for our example, the result in case (2) would have been 40 eV per electron, except for the fact that the assumed thermal equilibrium would be disrupted in such an extreme situation.) The case of helium is not so conveniently treated; however a few general conclusions may be reached. The upper states, at least, are hydrogen-like. The contribution to the absorption of the free-free transitions, which amounts to about 70% of the total absorption in the examples just considered, should also be very similar.

Since the density of free electrons should be very large compared to the populations of neutral atomic levels, no significant increase in the electron density can be expected. It is, of course, quite possible that the assumption of complete thermodynamic equilibrium

is not a good one for a laboratory plasma. A situation which has been observed in afterglows [II-18] is that the upper states of the atoms ($N \geq 6$) and the electron cloud are in equilibrium with each other, but the populations of the lower states diverge widely from their equilibrium values. In this case the calculation of free-free absorption will still be approximately valid, but if the population of the intermediate levels should be large, there is a possibility that substantial photoionization could take place. It is unlikely that the populations of the upper neutral states could ever be large enough to produce much change in the total electron density through sudden photoionization. However an interesting observation of photoionization caused by a long (~1 millisecond) normal laser pulse has been made by Rose, Lidsky and Thompson. [II-10] In this case it is thought that the density of neutrals in ionizable states is continuously replenished while photoionization is taking place, so that an equilibrium at an increased electron density is established. In order to avoid such effects, short laser pulses would be desirable.

Another possible mechanism by which the optical radiation could alter the density of the plasma is that of collisional ionization by electrons. This effect was first observed by Damon and Tomlinson [II-11] in various gases at a pressure of twenty microns, using both normal and giant-pulse lasers. The number of ions produced was on the order of $10^7$. Later studies by Minck [II-12] indicate that the process is most effective at pressures of many atmospheres, and that the mechanism is probably the same as that of microwave ionization, which is

interruption of the oscillatory motion of electrons by collisions, and statistical accumulation of energy on a random-walk basis. Multiple-photon absorption does not seem to be an important part of the process. Possibly the initial presence of electrons could enhance ion production by many orders of magnitude; it is not clear whether the equilibrium increase in density can be large enough to be significant. However, no signs of collisional ionization have been observed in the present work.

In addition to the processes which have already been mentioned, there is a wide spectrum of high-field effects which are only beginning to be understood. One particularly interesting case, that of Thomson scattering under conditions of high photon density, has been treated using quantum electrodynamics [II-13] by Fried. His result for the scattering amplitude is

$$A \cong A_o \, J_o \left( \underline{\varepsilon} \cdot \underline{k}' \sqrt{2e^2 h \, (m^2 c^3)^{-1} \, \rho\lambda} \right) \qquad \text{(II-21)}$$

where $A_o$ is the ordinary Thomson scattering amplitude, $\varepsilon$ is the unit vector in the direction of polarization of the incident beam, $k'$ the propagation vector of the scattered photon, $\rho$ the density of photons, and $\lambda$ is the incident wavelength. We see from Eq. II-21 that in this theory the scattering in directions perpendicular to the incident polarization has its classical value regardless of the photon density. Moreover, with existing lasers no significant deviations from classical behavior are to be expected at other angles. Many other papers on high-field effects have also been published, but as yet none

in which the effects are likely to be significant for scattering experiments such as are being described, has come to the attention of the writer.

D. Atomic Scattering

In addition to the scattering by free electrons, radiation will also be scattered by neutral atoms when these are present. It is expected that this effect, usually called Rayleigh scattering, can be used for calibration of electron scattering experiments, and so a brief review and discussion will be included.

In the macroscopic point of view, the volume polarization is related to the applied electric field by the index of refraction. If we are dealing with an isotropic medium (such as an inert gas) we can write

$$\underset{\sim}{P} = \underset{\sim}{E}\,(\epsilon - \epsilon_o) = \underset{\sim}{E}\,\epsilon_o\,(N^2 - 1) \qquad \text{(II-22)}$$

where $N$ is the index of refraction, and $\underset{\sim}{P} = n\underset{\sim}{p}$ is the density of atoms times their individual polarization. We now apply Eq. II-3 to the particles individually, which are regarded as oscillating dipoles $pe^{j\omega t}$. (Only the dipole radiation need be considered due to the atom's small dimensions.) When Eq. II-22 is substituted for p, and the scattered radiation is integrated over the sphere, we obtain the total scattering cross-section

$$\sigma = \frac{32}{3}\,\pi^3\,\lambda^{-4}\,n^{-2}\,(N-1)^2 \qquad \text{(II-23)}$$

where N is the index of refraction and n is the density of scatterers and the pressure at which N is measured. This equation, with its $\lambda^{-4}$ dependence, is the Rayleigh Scattering Law. [II-14]

The dependence of the intensity scattered at $90^{o}$ on the quantity $(N - 1)^2$ has been verified by Rayleigh for such diverse gases as air, hydrogen, nitrous oxide, and ether vapor, with errors of only a few per cent. [II-15] A more recent experimental study has been carried out by George et al, [II-16] using a normal, focused ruby laser as the light source. They report some rather peculiar results. Their differential cross-sections are in the range twice to three times those predicted by the Rayleigh formula; and in the scattering plane perpendicular to the incident electric vector, they do not observe the scattered intensity to be constant as a function of scattering angle, but rather to increase in the forward and backward directions. The authors have suggested that these departures from the Rayleigh theory *may result from some kind of coherence effect,* but no firm explanation has been established. [II-17] Further investigation is needed in order to determine if some such hidden mechanism will introduce error in density measurements.

There will also be scattering from the ions present in the plasma. The Thomson component of this scattering is reduced from that of free electrons by the factor $(m/M)^2$ and hence is negligibly small. In addition there will be scattering (identical with that of neutral atoms) due to two-photon processes. These may be expressed for both atoms and ions by the semi-classical formula

$$\sigma_{atom} = \sigma_o \left[ \sum_R f_R \frac{\omega^2}{\omega_R^2 - \omega^2} \right]^2 \qquad \text{(II-24)}$$

where the $\omega_R = (\Delta E)_R/\hbar$ for transitions to all other states $R$ of the atom, and the $f_R$ are the corresponding absorption oscillator strengths. If $\omega \ll \omega_R$ Eq. II-24 may be approximated by

$$\sigma_{atom} \cong \sigma_o \left( \frac{\hbar\omega}{\overline{\Delta E}} \right)^4 \left( \sum f_R \right)^2 \qquad \text{(II-25)}$$

where $\overline{\Delta E}$ is an "average" transition energy. The sum $\sum f_R$ is equal to the number of electrons in the atom or ion, by the Thomas-Kuhn-Reiche sum rule. Since for the ground state of an ion $\overline{\Delta E}$ will be much larger than for the ground state of a neutral atom, while $\sum f_R$ is smaller, it is evident that the scattering of an ion will be small compared to that of a neutral.

There does exist a remote possibility that in the chaos of a gas discharge, the upper levels of atoms or ions might somehow become heavily populated at the expense of the ground state. If this were to happen the quantities $\omega_R^2 - \omega^2$ in the denominator of II-24 would become smaller, and the scattering would be increased. However, reported intermediate level populations in the helium afterglow having densities $\sim 10^{13}$/cc are of the order of $10^9$/cc, [II-18] and only a most unlikely resonance situation could increase the atomic scattering to compete with the electron scattering. (No such resonance exists for the ruby laser in helium.)

## REFERENCES


II-1. J. J. Thomson, Conduction of Electricity Through Gases, 3rd edition, Cambridge, 1933, Vol. II, p.256.

II-2. See, for instance, L. Landau and E. Lifshitz, The Classical Theory of Fields, Addison-Wesley (1951), p.193.

II-3. C. H. Papas and K. S. H. Lee, The Incoherent Scattering of Electromagnetic Waves by Free Electrons, Calif. Institute of Tech. Antenna Laboratory Technical Report No. 26 (August 1961).

II-4. O. Buneman, Journal of Geophysical Research 67, 2050-53 (May 1962).

II-5. J. P. Dougherty and D. T. Farley, Proc. Roy. Soc. A 259, 79-99 (1960).

II-6. J. A. Fejer, Canadian Journal of Physics 38, 1114-1133 (1960).

II-7. E. E. Salpeter, Physical Review 120, 1528-35 (Dec. 1960).

II-8. W. H. Kegel, Proceedings of the Sixth Conference on Ionization Phenomena in Gases, Paris, 1963.

II-9. A. Unsoeld, Physik der Sternatmosphaeren, 2nd ed.; Springer, Berlin, (1955); pp.165-171.

II-10. D. J. Rose, L. M. Lidsky and E. Thompson, 5th Annual Meeting of A.P.S. Division of Plasma Physics, San Diego, Calif., (Nov. 1963); also E. Thompson, private communication.

II-11. E. K Damon and R. G. Tomlinson, Applied Optics 2, 546-547 (May 1963).

II-12. R. W. Minck, J. Appl. Physics 35, 252-254 (Jan. 1964).

II-13. Z. Fried, Physics Letters 3, 349-351 (Feb. 1963).

II-14. Lord Rayleigh, Philosophical Magazine 47, 375-84 (1899).

II-15. Lord Rayleigh, Proc. Royal Society 95, 155-70 (1918).

II-16. T. V. George, L. Slama, M. Yokoyama and L. Goldstein, Phys. Rev. Lett. 11, 403-406 (Nov. 1, 1963).

II-17. T. V. George and L. Goldstein, Scattering of Ruby Laser Light by Gases, AFCRL Report AFCRL-63-519; University of Illinois, Oct., 1963.

II-18. E. Hinnov and T. G. Hirschberg, Phys. Rev. 215, 795-801 (Feb. 1, 1962).

# CHAPTER III

# PHOTON-ELECTRON SCATTERING IN THE LABORATORY

## A. General Considerations

A photon-electron scattering experiment will typically consist of the following elements:

(1) a source of photons with a monitor if necessary

(2) a source of free electrons

(3) a chamber of some sort in which the interaction is to take place

(4) a detector for the scattered photons, which will register intensity, wavelength or both.

The two principal difficulties, which until very recently have made such experiments unattractive or impossible, are those of

(1) obtaining a light source of sufficient power and surface brightness to give a usable scattered signal intensity, while

(2) preventing spurious reflections from the walls of the apparatus from masking the very small scattered signal.

Actually the problems of the light source and the spurious wall reflections are interrelated. Because of the small value of the photon-electron (Thomson) cross-section $\sigma$ (which is $6 \cdot 10^{-25}\ cm^2$), it is seen that even disregarding all loss mechanisms, the usable scattering cross-section will be of the order of

$$\sigma_T = \sigma\, nV\Omega\, \sin^2 \theta \qquad \text{(III-1)}$$

where $\sigma_\tau$ is the total usable cross-section, n the free electron density, V the scattering volume, $\Omega$ the solid angle of acceptance of the detector, and $\theta$ the angle between the direction of observation and the direction of the electric vector of the incident (polarized) light. For such reasonable values as $n = 10^{14}/cc$, $V = 1$ cc, $\Omega = 10^{-2}$, $\theta = \frac{\pi}{2}$, one finds that $\sigma_\tau \sim 6 \cdot 10^{-13}$. Consequently the fraction of the incident light reaching the detector due to reflections from the apparatus walls must not be much in excess of one part in $10^{12}$, or else the light scattered by electrons will be drowned out. An evident precaution to forestall such wall reflections is to provide that the incident light shall pass through the apparatus in a nearly parallel beam without striking anything at all, until it has passed a considerable distance away from the detector (this prohibition includes glass windows and lenses, which may scatter 0.1% of the transmitted light). This places an important restriction on the source optics. Moreover, it will be shown that the incident light must be supplied in a narrow beam, in order that the scattering region may provide sufficient brightness for the detector optics. Let us evaluate these considerations, in order to arrive at light source requirements.

The appropriate configuration of the photodetector can be represented by a slit of length $\ell$, width 2w, parallel to the direction of the incident light. The detector optics accept light which makes an angle of less than $\alpha$ with its axis. The angle of observation will be taken as $90^\circ$ with respect to the incident beam, which is assumed to be uniform and circular in cross-section with radius $\rho$ in the scattering

region. Let us stipulate in addition that because of the requirement that the wall reflections be kept small, none of the source optics may be closer to the scattering region than a distance f, which experience indicates to be around 50 cm. The volume where a uniform ionization is present is considered to be much larger than the region of acceptance of the detector optics. The meanings of these quantities are illustrated in Fig. III-1, which shows a typical experimental arrangement. Here the detector is equipped with a collecting lens of radius R, the position of which is also indicated in the figure.

The ratio of power reaching the detector to incident power in this case (taking the dipole scattering pattern into account) is then

$$\frac{P_s}{P_i} = \frac{3}{4\pi} (n\sigma) \frac{\ell R\alpha}{b} \left[ \left(\frac{bw}{c}\right) \sqrt{1 - \left(\frac{bw}{c}\right)^2} + \sin^{-1} \left(\frac{bw}{c}\right) \right] \qquad \text{(III-2)}$$

for the case $\frac{bw}{c} \leq \rho$, and

$$\frac{P_s}{P_i} = \frac{3}{8} (n\sigma) \frac{\ell R\alpha}{b} \qquad \text{(III-3)}$$

for the case $\frac{bw}{c} \geq \rho$. Clearly it is desirable that $\frac{bw}{c} \geq \rho$, which may be rewritten $\frac{bw\alpha}{R} \geq 1$, as $\alpha c \cong R$. (This condition simply means that all power goes through the detector's region of acceptance and none around it. Power can of course be sent around it also; then that power is simply wasted and need not be considered.) Let us assume that w and $\alpha$ are given values for a suitable spectrometer; R is to be kept as large as convenient, and b is to be kept as small as convenient

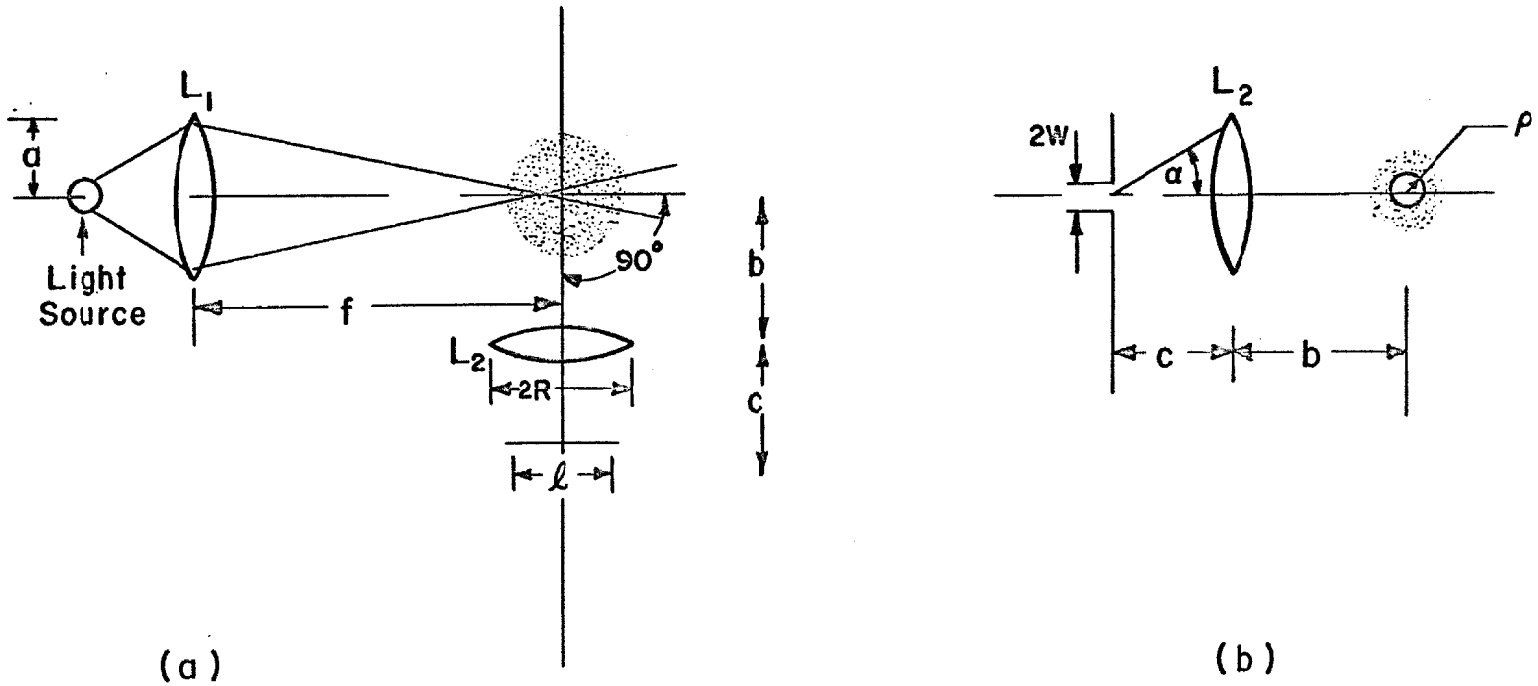


Figure III-1: Hypothetical Scattering Experiment. (a) View perpendicular to scattering plane (b) View parallel to scattering plane.

since from Eq. II-3 the scattered power is proportional to $R/b^2$. This gives a maximum value for $\rho$:

$$\rho < \frac{bw\alpha}{R} \qquad \text{(III-4)}$$

In this case Eq. II-3 will apply. As we proceed, let us parenthetically consider specific numbers in order to suggest orders of magnitude. Inserting the values $n = 10^{14}$/cc, $\sigma = 6 \cdot 10^{-25}$ cm$^2$, R = 2.5 cm, $\alpha = \frac{1}{9}$ radian, $\ell$ = 1 cm, b = 10 cm, we obtain

$$P_s = 2.4 \cdot 10^{-13} \; P_i \qquad \text{(III-5)}$$

The question next to be considered is, what constitutes an acceptable signal level $P_s$? This will depend on the conditions of the experiment, particularly on whether it is carried out on a pulsed or continuous basis. Let us suppose the most favorable situation, that we have a monochromatic light source which we can operate continuously, using a synchronous detection system. Then the limiting factor on $P_s$ will probably be the background luminosity of the plasma. Calculations of the emissivity of a fully ionized equilibrium hydrogen plasma have been carried out by Berman, [III-1] who finds that in the spectral range 2-3 eV, the emissivity E of such a plasma having density $10^{14}$/cc and temperature 3 eV will be $2.7 \cdot 10^{-4}$ watts/cc. If we take the slit width w to be 100 microns, and the plasma is k cm deep as seen by the detector, then the power reaching the detector from plasma luminosity is

$$P_L = E \frac{kw\ell\alpha^2}{4} \qquad \text{(III-6)}$$

If $k = 1$ cm, $P_L = 7 \cdot 10^{-9}$ watt. The signal power which can be detected by a synchronous detector under these conditions can be estimated by finding the shot noise power within its bandwidth. If the bandwidth, B, is one cycle, and the quantum efficiency is $10^{-2}$, a signal $P_s = 4 \cdot 10^{-13}$ watt would give a one-to-one signal-to-noise ratio. From Eq. III-5 we find that we require $P_i = 1.7$ watt.

We shall now establish the requirements on the light source in terms of its surface brightness. It is easily shown from geometrical optics that the intensity at the image of a Lambert's-law light source having surface brightness B, is

$$I = \frac{Ba^2}{f^2} \qquad \text{(III-7)}$$

where a is the radius of the lens producing the image and f is the distance from the lens to the image (see Fig. III-1). Using III-4 we obtain

$$I = \frac{P_i}{\pi\rho^2} = \frac{P_i R^2}{\pi b^2 w^2 \alpha^2} = \frac{Ba^2}{f^2}$$

$$B = P_i \frac{f^2 R^2}{\pi a^2 b^2 w^2 \alpha^2} \qquad \text{(III-8)}$$

Values for all quantities on the right of Eq. III-8 have been suggested except for a, which we can take as 1 cm; we find that the minimum

source brightness would be $1.4 \cdot 10^7$ watts/cm$^2$.

Perhaps the brightest laboratory source of incoherent light now available is the PEK labs super high pressure mercury arc lamp; the brightness of this lamp over the entire visible spectrum is 250 watts/cm$^2$. Even if one takes the trouble of using the surface of the sun as the light source it would be insufficient; the brightness of the sun is only about 2500 W/cm$^2$. This analysis shows why the use of incoherent sources is unpromising.

Recently, however, the advent of the laser has provided us with a light source of phenomenal brightness. It has been shown using the Kirchoff integral, that for a laser of power $P$ in a single $TEM_{00}$ mode, the maximum intensity that can be produced when the light is brought to a focus is

$$I_{max} = 2.60\ P\ \left(\frac{f\lambda}{a}\right)^{-2} \qquad \text{(III-9)}$$

where $\lambda$ is the wavelength and the other symbols have their previous meanings. [III-2] The laser is not, of course, a Lambert's-law source; however, in order to compare it with incoherent sources, it will be meaningful to consider an equivalent brightness $B'$ defined by the use of Eqs. II-9 and II-7. Thus

$$B' = 2.60\ P\ \lambda^{-2} \qquad \text{(III-10)}$$

There are available on the market helium-neon gas-phase lasers producing $5 \cdot 10^{-3}$ watts at 6328Å in a single mode. The equivalent brightness of

such a laser is $3.35 \cdot 10^6$ watts/cm$^2$. In addition to being extremely bright, the laser light source is also nearly monochromatic and coherent, which opens an additional range of possibilities. Because of the laser's monochromaticity, spectral analysis of the scattered light may be performed. Moreover, because of the narrow spectral width of the returned light, much of the broadband plasma luminosity can be eliminated.

Let us calculate the requirements on a cw laser light source for a scattering experiment. Using formulas III-3, III-6, III-8, and the Schottky shot-noise formula, we can eliminate the slit width w, and calculate the power required from a source of given brightness for one-to-one signal-to-noise ratio:

$$P_i^{\frac{3}{2}} B^{\frac{1}{2}} = \frac{1}{(n\sigma)^{\frac{1}{2}}} \frac{32}{9\pi^{\frac{1}{2}}} \frac{befk\, E(\Delta\lambda)\mathcal{B}}{a\alpha\ell R\,(\epsilon Q)} \qquad \text{(III-11)}$$

where $\mathcal{B}$ is the synchronous detector bandwidth, E the plasma emissivity in watts/cm$^3$angstrom, $\Delta\lambda$ the optical bandwidth, e the electronic charge and $(\epsilon Q)$ the effective quantum efficiency of the photocathode. Physically, the meaning of this formula is as follows: if the source is bright, the width of the scattering region, proportional to w, can be reduced. Then less plasma is within the detector's region of acceptance and less power is required to overcome the luminosity. Using Eq. III-10 we find that the minimum power of the gas laser is given by

$$P^2_{(min)} = 1.24 \frac{1}{(n\sigma)^2} \frac{befk\, E(\Delta\lambda)\mathcal{B}\lambda}{a\alpha\ell R\,(\epsilon Q)} \qquad \text{(III-12)}$$

Thus if the experiment is arranged as described above, and $(\Delta\lambda)$ is 10 Angstroms, $\mathcal{R}$ is one cycle, $\lambda = 6000\text{Å}$, $(\varepsilon Q) = 10^{-2}$, and Berman's value for the emissivity is used, the minimum ac laser power is approximately 40 milliwatts.

In addition to the mode of operation described above, the cw laser offers the possibility of detection by optical mixing, as has been done by Cummins, Knable and Yeh.[III-3] In this technique a fraction of the incident light from the laser is diverted and mixed with the scattered light at the photocathode, creating what is essentially an optical superheterodyne receiver. Such a receiver can have a tunable bandwidth on the order of a few cycles, compared with the order of $10^{11}$ cycles if the detector is tuned by means of a grating spectrometer. The photodetector can have a large aperture (instead of a spectrometer entrance slit) and an angle of acceptance of $\frac{\pi}{2}$. These features, however, are not particularly useful in plasma scattering experiments. Because of the inefficiency of the optical mixing process it is doubtful that any increase in sensitivity can be gained, nor can the wider aperture be used effectively, since increased plasma luminosity noise will result. Moreover the Doppler shifts resulting from moderate electron thermal velocities will result in intermediate frequencies that are inconveniently high.

The brightest light source of any kind that is now available is the "giant-pulse" ruby laser (see Appendix). This device is capable of producing more than one megawatt of energy at 6943Å with duration on

the order of $5 \cdot 10^{-8}$ second. Assuming that one one-hundredth the power is in the $TEM_{00}$ mode we find an equivalent brightness of $B' = 5.4 \cdot 10^{12}$ watts/cm$^2$, roughly one billion times the brightness of the sun! However because the giant-pulse laser is useful only on a pulse basis, the computations of signal-strength above, based on synchronous detection, do not apply. Signal-to-noise considerations in pulsed scattering experiments will be discussed in the following section.

## B. Noise Considerations in Pulsed Scattering Experiments

In the previous section some general comments on signal levels in scattering experiments were presented, using as an example a case in which both plasma and light source were constant in time. We now consider the case in which the light source is a giant-pulse ruby laser supplying a light pulse some fifty nanoseconds in duration. The detector, in this case, will receive a burst of scattered light superimposed on the background plasma luminosity (which may now also be varying in time; in most cases the variation will be very slow compared with that of the incident pulse). At first thought, one might suppose that the limitation on signal strength in this case is reached when the scattered signal becomes smaller than the "dc" background signal; however, the background signal current is not in fact dc, but contains shot noise, and it is the shot noise which presents the limitation. Additional difficulty in measurement arises from the fact that the scattered-signal current itself contains shot noise.

Two different expressions for the signal-to-noise ratio of an electron multiplier are found in the literature; these are based on two different fundamental conceptions of the secondary emission process. In practice the difference between the two is not very important, since the greatest part of the noise is introduced not in the multiplier but at the photocathode.

The first point of view is that secondary electrons are emitted in such a way that for each primary electron the number of secondaries is given by the Poisson distribution. This postulate first arose from the early experiments of Hall and Williams [III-4] and seems to have been perpetuated by its inclusion in Zworykin's paper describing the photomultiplier tube. [III-5] If the postulate is correct, then one can justify the following assumptions:

(1) Secondary emission from any anode follows the shot-effect law, $\overline{\Delta i_s^2} = 2 e \mathcal{B} i_s$, where $i_s$ is the average emitted secondary current, $e$ the electronic charge and $\mathcal{B}$ the bandwidth;

(2) Shot noise from any anode is multiplied by subsequent stages in the same way as the signal is.

One then finds by straightforward calculation that for a dynode chain having any number $k$ of dynodes,

$$(S/N)_{out} = (S/N)_{in} \frac{\bar{n} - 1}{n} \qquad \text{(III-13)}$$

where $(S/N)$ are input and output signal-power-to-noise ratios, $\bar{n}$ is the average dynode multiplication factor (assumed the same for all

dynodes), and $\bar{n}^{(k+1)}$ is assumed much greater than one. [III-6]

While formula III-13 is to be found nearly everywhere in the literature, the fundamental assumption is not only difficult to justify, but not even well supported by later experiments. An altogether more satisfactory (but less known) theory is that of Shockley and Pierce. [III-7] They stated that the multiplication factor n is a statistical quantity, described by the statement that the fraction of primary electrons multiplied by the factor n is $\beta_n$. Thus

$$\sum_{n=0}^{\infty} \beta_n = 1 \qquad \text{(III-14)}$$

and

$$i_p \sum_{n=0}^{\infty} n \beta_N = i_s$$

where $i_p$ and $i_s$ are the average multiplier input and output currents. Each group of electrons corresponding to an integer value of n contributes to the noise current a fluctuation which is the same as would be produced by its current $i_n$ if composed of "large" electrons each having charge ne. Thus this contribution is

$$\overline{(I_n - i_n)^2} = 2ne\, i_n \mathcal{B} = 2n^2 e \beta_n i_p \mathcal{B} \qquad \text{(III-15)}$$

where $I_n$ is the instantaneous current. The total mean-square fluctuation is obtained by adding the squares of its parts:

$$\overline{(I_s - i_s)^2} = \sum_{n=0}^{\infty} \overline{(I_n - i_n)^2} = 2ei_p \mathcal{B} \sum_{n=0}^{\infty} n^2 \beta_n \qquad \text{(III-16)}$$

Evidently

$$2\, e\, i_p\, \mathfrak{B} = \overline{(I_p - i_p)^2} \equiv \overline{\Delta i_p^{\,2}} \qquad \text{(III-17)}$$

$$\sum_{n=0}^{\infty} n^2\, \beta_n = \overline{n^2} = (\bar{n})^2 + \sigma^2 \qquad \text{(III-18)}$$

where $\sigma^2$ is the variance of the multiplication process. Substituting these relations gives

$$\overline{\Delta i_s^{\,2}} = \bar{n}^2\, \overline{\Delta i_p^{\,2}} + \sigma^2\, \overline{\Delta i_p^{\,2}} = 2\, e\, i_p\, \mathfrak{B}\, (\bar{n}^2 + \sigma^2) \qquad \text{(III-19)}$$

Thus the noise current from the multiplier is the noise current input times the average multiplication, plus another contribution having to do with the irregularity of the multiplication process. The same result can be obtained by calculating directly the autocorrelation function of the sum of the individual electron currents. [III-8]

From Eq. III-19 it is easily shown that for a sequence of identical dynodes having overall gain $g$ large compared to one,

$$\overline{\Delta i^2}_{out} = \overline{\Delta i_p^{\,2}}\; g^2 \left(1 + \frac{\sigma^2}{\bar{n}\,(\bar{n} - 1)}\right) \qquad \text{(III-20)}$$

The quantity $\sigma^2$ is of course strongly dependent on the experimental conditions. (Reduction of Zworykin's measurements gives a value of $\sigma^2 = \frac{1}{4}\,\bar{n}^2$. [III-9]) Let us denote the quantity in parentheses in Eq. III-20 by the letter C, thus:

$$C = 1 + \frac{\sigma^2}{\bar{n}\,(\bar{n} - 1)} \qquad \text{(III-21)}$$

Putting this into a form which can be compared with Eq. II-13 we obtain

$$(S/N)_{out} = (S/N)_{in}\, C^{-1} \qquad \text{(III-22)}$$

In the photomultiplier the input current fluctuation is simply

$$\overline{\Delta i_p^2} = 2e\, \epsilon i_c \mathcal{B} \qquad \text{(III-23)}$$

where $i_c$ is the average photocurrent and $\epsilon$ is the fraction of photoelectrons captured by the first dynode. Combining Eqs. III-20 and III-23 gives

$$\overline{\Delta i^2}_{out} = 2e\, \epsilon\, \mathcal{B} g^2\, C i_c \qquad \text{(III-24)}$$

as the final result to be obtained from the Shockley-Pierce theory. Eq. III-24 will be employed in what follows. (Note that if a Poisson distribution is assumed, so that $\sigma^2 = \bar{n}$, then III-24 reduces to III-13.)

We shall now derive a signal-to-noise ratio for a pulsed scattering experiment. Assume that the photocurrent $i_c$ is composed of $i_L$, which arises from the plasma luminosity and is slowly varying, and $i_e$, which comes from light scattered by electrons. A measurement can consist of measuring the value of $\epsilon g(i_e + i_L)$ at the instant when the laser output is known to be greatest, and subtracting a measurement

of $\epsilon g i_L$ at the same time in the development of the discharge. Both measurements are drawn from independent gaussian distributions, the first having standard deviation $g\left[K(i_e + i_L)\epsilon\right]^{\frac{1}{2}}$ and the second $g\left[K i_L \epsilon\right]^{\frac{1}{2}}$, where $K$ is the constant $2e\mathfrak{B}C$. The standard deviation of the measurement is thus $\epsilon^{\frac{1}{2}} g K^{\frac{1}{2}} (i_e + 2i_L)^{\frac{1}{2}}$. The expectation value of the measurement is $\epsilon g i_e$; hence if we define a signal-to-noise ratio $R$ such that $R$ equals the expectation value of the measurement divided by the standard deviation of the measurement, we have

$$R = \frac{\epsilon^{\frac{1}{2}} i_e}{K^{\frac{1}{2}} (i_e + 2i_L)^{\frac{1}{2}}} \qquad \text{(III-25)}$$

The result (III-25) is based on the tacit assumption that the detector is equipped with a filter which gives virtually undistorted response for frequencies less than $\mathfrak{B}$, and high attenuation for frequencies greater than $\mathfrak{B}$. In practice this is the amplifier of the oscilloscope. One might expect that a better signal-to-noise ratio could be obtained by a suitable filter, such as a gating circuit followed by an RC network. In fact it can be shown that if the signal pulse is square and the shot noise is "white", the best result is obtained from a perfect integrator. Let us suppose that the photomultiplier output is gated and applied to a circuit whose impulse response is $h(t)$. The response to a square current signal pulse of magnitude $\epsilon g i$ and duration $T$, at times $t \geq T$, is

$$s(t) = \epsilon g i \int_0^T h(t - x)\, dx \qquad \text{(III-26)}$$

The signal will be assumed to have white shot noise imposed on it, and we now find the variance for a measurement of $s(t)$ corresponding to noise with spectral density $S(\omega) = (2\pi)^{-1}\ e\epsilon g^2\ Ci$ :

$$\sigma^2 = E\left[\int_0^T h(t - x)\ f_i(x)\ dx \int_0^T h(t - y)\ f_i(y)\ dy\right] \qquad \text{(III-27)}$$

where $f_i(t)$ is the random process noise input to the circuit and $E$ is the expectation value operator. We then have

$$\sigma^2 = \int_0^T h(t - x)\ dx \int_{-x}^{T-x} h(t - x - \tau)\ R(\tau)\ d\tau \qquad \text{(III-28)}$$

where $R$ is the autocorrelation function, which we take to be $R(\tau) = e\epsilon g^2\ Ci\ \delta(\tau)$. For convenience let us assume that the measurement will be made immediately after the optical pulse has ended, that is, at $t = T$. Then we have

$$\sigma^2 = e\epsilon g^2\ Ci \int_0^T \left[h(x)\right]^2 dx \qquad \text{(III-29)}$$

For a single piece of scattering information we shall need two measurements: first one of signal plus plasma luminosity $(i = i_e + i_L)$, and then, to subtract from it, a measurement of the luminosity only $(i = i_L)$. (If the plasma is non-reproducible the measurements are conveniently made simultaneously by two photomultiplier tubes.) Defining a signal-to-noise ratio analogously to Eq. III-25, we obtain

$$R = \frac{s}{\sigma} = \frac{e^{\frac{1}{2}}}{e^{\frac{1}{2}} C^{\frac{1}{2}}} \frac{i_e}{(i_e + 2i_L)^{\frac{1}{2}}} \frac{\int_0^T h(x)\, dx}{\left[\int_0^T h(x)^2\, dx\right]^{\frac{1}{2}}} \qquad \text{(III-30)}$$

The choice of the function $h(x)$ which will maximize $R$ is that of $h(x) = \text{constant}$. This implies that the detection circuit should be a perfect integrator. In practice it may be convenient to use a load consisting of a resistance $r$ in parallel with the capacitor $c$. If the time-constant $rc$ is called $\theta$, we substitute $h(t) = \frac{1}{c} e^{-\frac{t}{\theta}}$ into Eq. III-30, obtaining

$$R = \frac{(2\epsilon)^{\frac{1}{2}}}{(eC)^{\frac{1}{2}}} \frac{i_e}{(i_e + 2i_L)^{\frac{1}{2}}} \frac{\theta^{\frac{1}{2}} (1 - e^{-\frac{T}{\theta}})}{(1 - e^{-2\frac{T}{\theta}})^{\frac{1}{2}}} \qquad \text{(III-30A)}$$

Regarded as a function of a normalized bandwidth $(\frac{T}{\theta})$, $R$ is monotonically decreasing. The low bandwidth limit, corresponding to ideal integration, is

$$\lim_{\frac{T}{\theta} \to 0} R = \frac{e^{\frac{1}{2}}}{(eC)^{\frac{1}{2}}} \frac{i_e}{(i_e + 2i_L)^{\frac{1}{2}}} (T)^{\frac{1}{2}} \qquad \text{(III-31)}$$

The limit for $(\frac{T}{\theta}) \to \infty$ is zero; however, $R$ is still greater than 90% of its maximum at $(\frac{T}{\theta}) = 1$, and so any time constant greater than $T$ will suffice. This may be important if signal strength is low, as

the signal amplitude is proportional to $c^{-1}$.

It is interesting to compare the result III-31 with the result III-25 obtained for the case of an instantaneous peak measurement. If we take the bandwidth $\beta$ as $(2T)^{-1}$ so as to distort the pulse only slightly, III-25 becomes

$$(R)_{inst.} = \frac{e^{\frac{1}{2}}}{(2eC)^{\frac{1}{2}}} \frac{i_e}{(i_e + 2i_L)^{\frac{1}{2}}} (T)^{\frac{1}{2}} \qquad \text{(III-32)}$$

which is the same as for the integrated measurement, except for a factor of $(2)^{\frac{1}{2}}$. An additional consideration which favors integration, however, is that if instantaneous measurements are made with restricted bandpass, the rise times of the signal pulses (which vary slightly from one pulse to another) may affect the peak response.

Variations on the above two measurement schemes are of course possible. One may wish to integrate the noise only or the signal only, as convenient. Further improvement of the signal-to-noise ratio may be possible through the use of a filter designed with the consideration that the signal pulse is not really square. In that case the noise will vary with the signal in a complicated way; presumably an optimum filter can be designed if the exact shape of the signal pulse is known (possibly it could be derived from the monitor phototube). It would appear, however, that little is to be gained from further refinement in this direction. The most effective method of gating the incoming signal would be by means of an electronic switch actuated by the monitor phototube. An alternative scheme, used by Funfner, Kronast and Kunze, [III-10] makes use of two photomultipliers, one detecting signal plus

luminosity, the other luminosity only; the outputs of the tubes are then subtracted electronically. This method is useful if the plasma luminosity is large and non-reproducible; however because of shot noise and phototube imbalance Funfner et al were unable to reduce the bandwidth below one megacycle.

Let us now point out a few interesting applications of Eq. III-25 or III-31. First consider a case in which the electron density $n$ of the scattering plasma is increased without limit. It is clear that the scattered signal will increase in proportion to $n$, while (at least for an ideal plasma) the luminosity increases in proportion to $n^2$. [III-1] Nonetheless, replacing $i_e$ by $n$ and $i_L$ by $n^2$ in Eq. III-25 and taking the limit as $n \to \infty$, we find

$$\lim_{n \to \infty} R = \frac{\epsilon^{\frac{1}{2}}}{2 K^{\frac{1}{2}}} \qquad \text{(III-33)}$$

Thus one does not necessarily expect to encounter an upper limit on the density of the plasma to be diagnosed.

Next suppose that $i_L$ is large compared with $i_e$. Then if the total energy of the laser pulse $(\propto i_e T)$ is kept constant, but the peak power $(\propto i_e)$ is increased and $T$ reduced, an improvement in signal-to-noise ratio is expected from Eq. III-31.

Suppose that a filter transmitting 10% is placed before the photodetector, attenuating both signal $i_e$ and plasma luminosity current $i_L$ by this factor. We see from Eq. III-25 that the signal-to-noise ratio is decreased by $(10)^{-\frac{1}{2}} = 32\%$.

An obvious suggestion for improving the signal-to-noise ratio is that of placing a polarizer before the detector, in order to discriminate against the unpolarized plasma luminosity (the scattered light at $90^\circ$ being, of course, completely polarized). Measurements made at the ruby laser wavelength on a high-quality Polaroid HN-32 polarizer show that the maximum transmission for polarized light is 72% and that the transmission for unpolarized light is 38%. Multiplying $i_e$ and $i_L$ by these fractions, we find that $R'$, the new value of $R$, is

$$R' = \frac{.72\, i_e}{(.72\, i_e + .76\, i_L)^{\frac{1}{2}}} \qquad \text{(III-34)}$$

Let us consider the ratio $R'/R$ as a function of a parameter $p$, defined by $i_L = p i_e$. Then

$$R'/R = .72 \left(\frac{1 + 2p}{.72 + .76p}\right)^{\frac{1}{2}} \qquad \text{(III-35)}$$

When $p = 0$, $R'/R = .85$. When $p \to \infty$, $R'/R \to 1.16$. The case $R' = R$ obtains when $p = .71$. Thus whether or not an improvement is obtained from using a polarizer depends on the signal levels involved. With the HN-32 polarizer, the improvement is never very great.

As a final application of photomultiplier noise theory we shall now discuss an experimental situation in which two photomultipliers are used, one as detector for the scattered light as discussed above, the other as a monitor to meter the peak power of the incident light. In making measurements of the scattered light it is of course desirable to normalize to unit incident light intensity; the evident way of doing

this is to divide the one measurement by the other. Let us call the peak output of the scattered light detector $v_1$ and that of the monitor $v_2$. The two quantities are independent random variables with gaussian probability density functions $p_1$ and $p_2$, having mean values $a_1$ and $a_2$ and standard deviations $\sigma_1$ and $\sigma_2$. The quantity being measured is the ratio of scattered to incident light, given by the random variable $v_1/v_2$, which we shall call $x$. We shall now discuss the statistics of measurements of $x$.

First it is necessary to find the probability density function of $x$. Referring to the sketch of the $v_1 - v_2$ plane, Fig. III-2, we see that the domain of $x < 1$ is represented by the shaded area, and the corresponding probability $P(x < 1)$ is thus

$$\iint p_1(v_1)\, p_2(v_2)\, dv_1\, dv_2 \qquad \text{(III-36)}$$

integrated over that area. Let us assume at the outset that $a_2/\sigma_2$ is greater than, say, 1.7; this condition guarantees that more than 99% of the total probability lies in the right-half-plane, and consequently the contribution from the left half will be neglected. The probability distribution function is

$$P(x) = \int_{v_2=0}^{\infty} \int_{v_1=-\infty}^{xv_2} p_1(v_1)\, p_1(v_2)\, dv_1\, dv_2$$

$$= (2\pi\sigma_1\sigma_2)^{-1} \int_{v_2=0}^{\infty} \int_{v_1=-\infty}^{xv_2} e^{-\frac{(v_2-a_2)^2}{2\sigma_2^2}}\, e^{-\frac{(v_1-a_1)^2}{2\sigma_1^2}}\, dv_1\, dv_2 \qquad \text{(III-37)}$$

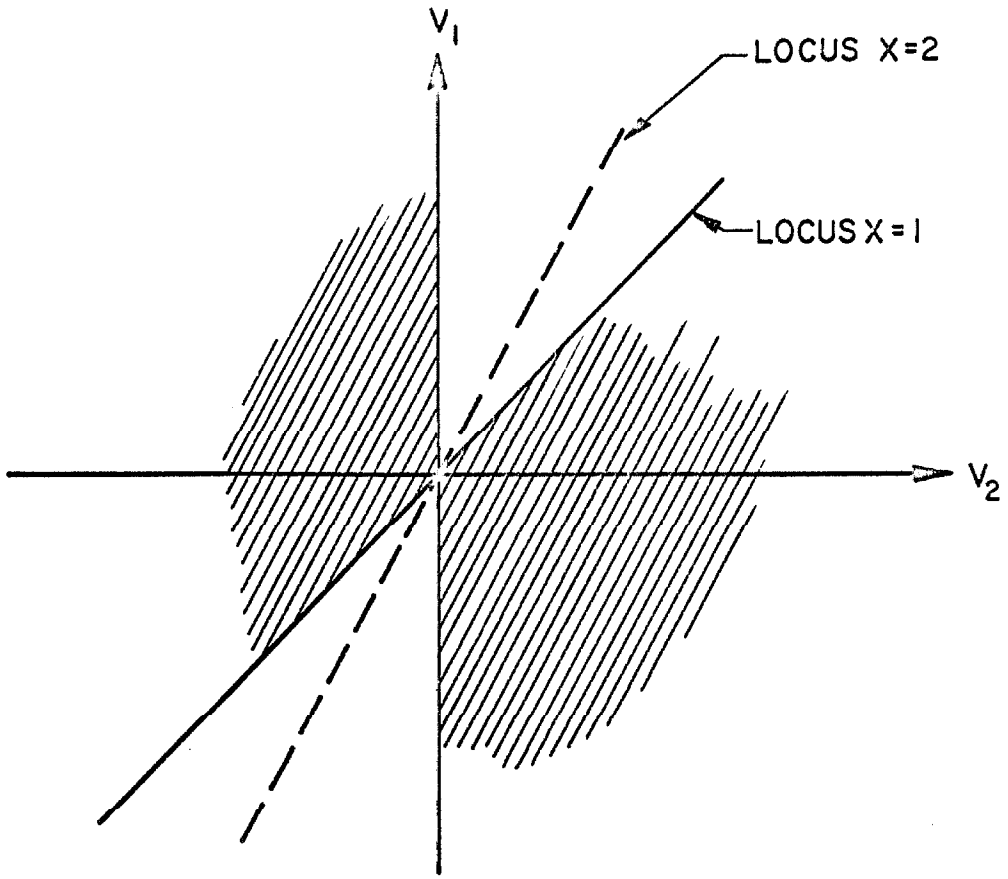


Figure III-2: Sketch of plane $v_1 - v_2$. Shaded area is region of $x < 1$.

and the probability density function of $x$ is

$$p(x) = \frac{d}{dx} P(x)$$

$$= (2\pi\sigma_1\sigma_2)^{-1} \int_0^\infty v_2 \exp\left\{ -\left[\sigma_1^2 \sigma_2^2\right]^{-1}\left[v_2^2(\sigma_1^2 + \sigma_2^2 x^2)\right.\right. \qquad \text{(III-38)}$$

$$\left.\left. - v_2(2a_2\sigma_1^2 + 2a_1\sigma_2^2 x) + (\sigma_1^2 a_2^2 + \sigma_2^2 a_1^2)\right]\right\} dv_2$$

To save writing let us define

$$\begin{aligned} (a_2\sigma_1^2 + a_1\sigma_2^2 x) &= f(x) \\ (\sigma_1^2 + \sigma_2^2 x^2) &= g(x) \end{aligned} \qquad \text{(III-39)}$$

Carrying out the integration we obtain

$$p(x) = \exp\left[-\tfrac{1}{2}(a_2^2\sigma_2^{-2} + a_1^2\sigma_1^{-2})\right] \left\{(2\pi)^{-1}\sigma_1\sigma_2 g^{-1}\right.$$

$$\left. + (8\pi)^{-\frac{1}{2}} g^{-\frac{3}{2}} f\left[1 + E_2(f\sigma_1^{-1}\sigma_2^{-1}2^{-\frac{1}{2}}g^{-\frac{1}{2}})\right]\exp\left[f^2(2g\sigma_1^2\sigma_2^2)^{-1}\right]\right\} \qquad \text{(III-40)}$$

where $E_2(u) = 2\pi^{-\frac{1}{2}} \int_0^u \exp(-t^2)\, dt$, following the notation of Jahnke and Emde. If $a_1 > 2\sigma_1$ and $a_2 > 2\sigma_2$ a good approximation is

$$p(x) \cong e^{-\frac{1}{2}\left(\frac{a_2^2}{\sigma_2^2} + \frac{a_1^2}{\sigma_1^2}\right)} (2\pi)^{-\frac{1}{2}} f g^{-\frac{3}{2}} \; e^{\frac{f^2}{2g\sigma_1^2\sigma_2^2}} \qquad \text{(III-41)}$$

In order to see physically what these equations represent, let us particularize to the especially simple case $a_1 = a_2 = a$, $\sigma_1 = \sigma_2 = \sigma$. Now the approximate result for $a > 2\sigma$ in Eq. III-41 becomes

$$p(x) \cong \frac{a}{\sigma(2\pi)^{\frac{1}{2}}} \; \frac{x+1}{(x^2+1)^{\frac{3}{2}}} \; e^{-\left(\frac{a}{\sigma}\right)^2 \frac{1}{2}\left(\frac{x^2 - 2x + 1}{x^2 + 1}\right)} \qquad \text{(III-42)}$$

The function appearing in Eq. III-42 is plotted in Fig. III-3, for the cases $a/\sigma = 2$ and $a/\sigma = 7$.

It will be seen that $p(x)$ has certain rather curious properties. For the case $a/\sigma = 2$, the most probable value of $x (\equiv v_1/v_2)$ is not one, even though the mean values of $v_1$ and $v_2$ are the same. Moreover, the mean value of $p(x)$ not only fails to be unity, but fails to exist, as the integrals for all moments of one or higher do not converge. Thus if one is measuring $x$, it is useless to take the average of many measurements; while if one adopts the most frequently recorded value, the number thus obtained will be incorrect. As $a/\sigma$ increases to seven the probability density function becomes narrower and its maximum moves toward $x = 1$; however, the mean value does not exist for any value of $a/\sigma$.

From the above it is evident that there is considerable danger of error in using a photomultiplier as a laser monitor. Such difficulty

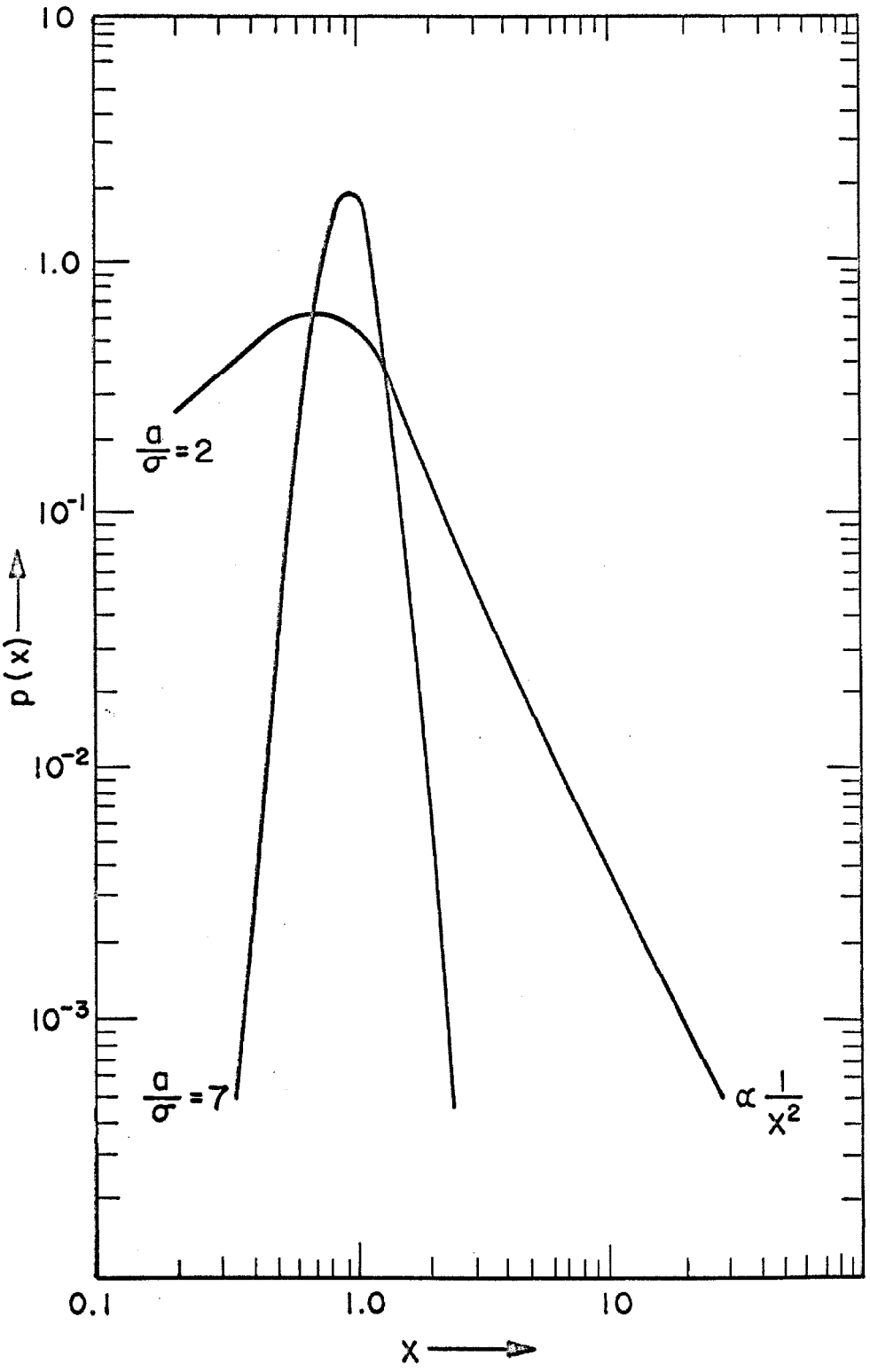


Figure III-3: p(x) from Eq. III-42.

can be easily avoided by the use of a high-current photodiode instead. Since the cathode current of the monitor will then be many orders of magnitude larger, the quantity $a_2/\sigma_2$ will become very large, and in this limit we obtain from Eq. III-41

$$\lim_{\sigma_2 \to 0} p(x) = \frac{1}{2\pi} \frac{a_2}{\sigma_1^2} e^{-\frac{1}{2}\frac{(x - a_1/a_2)^2}{(\sigma_1/a_2)^2}} \qquad \text{(III-43)}$$

so that the probability density is seen to approach the expected gaussian form. (It is true, that for any value of $a_2/\sigma_2$ less than infinity, the mean value still fails to exist. However as the limit $\sigma_2 = 0$ is approached, the probability that any individual measurement will not be drawn from the part of the distribution which is gaussian approaches zero.)

## C. Design and Construction of a Scattering Experiment

The principles outlined in the previous two sections have been put into practice in the construction of a pulsed scattering experiment. Since at the time work was begun no laboratory Thomson scattering of any kind had been reported, the design which was settled upon was one which would be most likely to demonstrate feasibility of the method. Great care was given to the questions of plasma luminosity, scattering by neutral atoms, and, particularly, to the reduction of unwanted wall reflections. The results have shown the design to be superior to all others which have appeared in terms of reduction of spurious scattering,

although certain shortcomings have become apparent.

Construction of related experiments, for the purpose of observing scattering of light by gases, was undertaken by Lord Rayleigh, [III-11] and recently by George, Slama, Yokoyama and Goldstein; [III-12] and free-electron scattering experiments have been reported by Thompson and Fiocco [III-13] and by Funfer, Kronast and Kunze.[III-10] George et al were unable to separate the scattering of hydrogen or helium from the wall reflections, while in the experiments of Thompson and Fiocco and of Funfer et al, the spurious reflections from the walls were so troublesome that no measurements could be made near to the laser wavelength. Both groups were forced to rely on the Doppler broadening of the returned signal, tuning the detector away from the center wavelength and subtracting out the component of the wall reflections which is transmitted by the detector's skirt selectivity. Under such conditions the spectrum of the returned signal is very difficult to determine. In the apparatus to be described here less than one part in $10^{14}$ of the incident light is received at the detector through wall reflections. Scattering from helium at atmospheric pressure is easily seen, and in plasma scattering experiments very little correction has to be made for spurious reflections.

A general diagram of the apparatus is given in Fig. III-4 and photographic views appear in Figs. III-5 and III-6. Light from the laser is focused on a .030" diameter pinhole for collimation and then passes through a second lens which again produces a converging beam, the focus of which is not directly before the detector. (About one-half

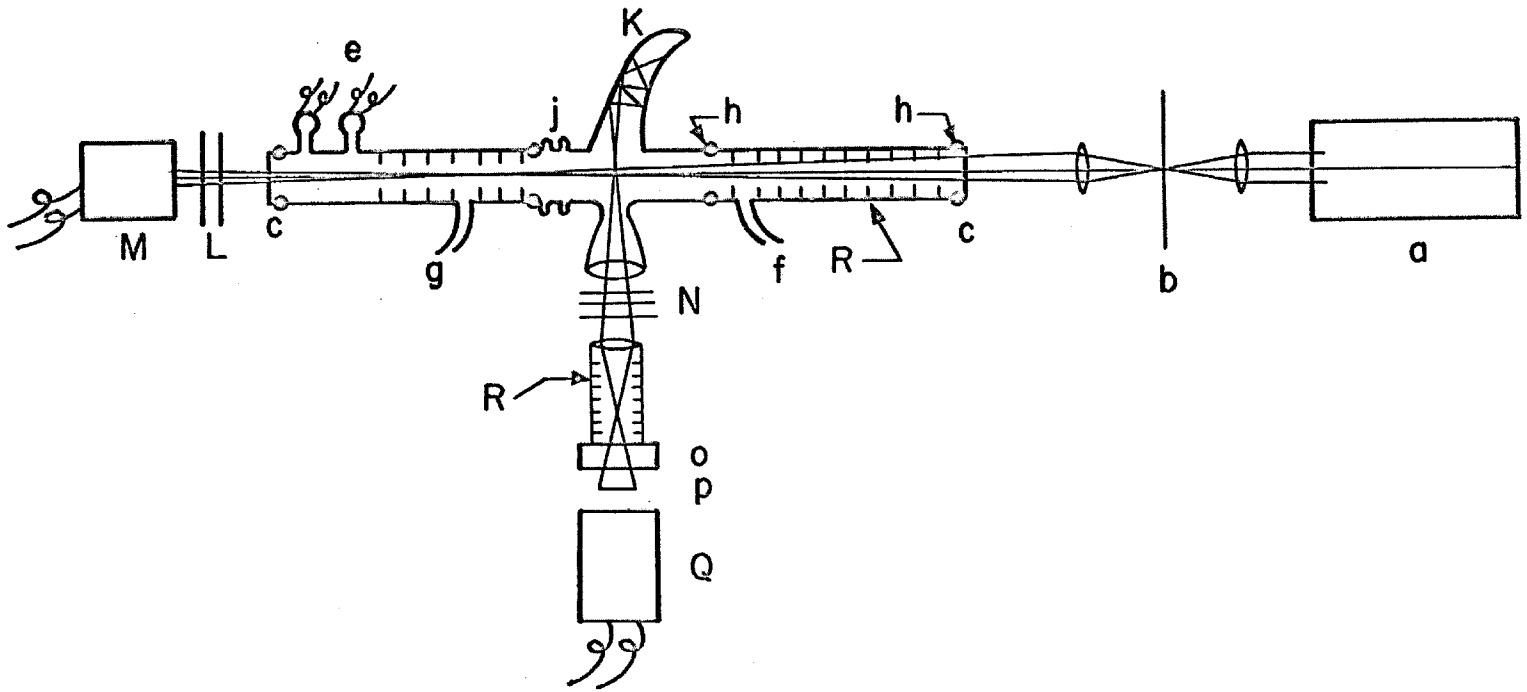


Figure III-4: Diagram of scattering experiment.
Key: a, giant pulse laser; b, pinhole; c, Brewster's-angle window; e, thermocouple vacuum gauges; f, helium inlet; g, outlet to sorptive trap and mechanical pump; h, glass-to-metal seals; j, bellows; k, Rayleigh horn; L, attenuators; m, photodiode monitor; n, filters and polarizer; o, tiltable interference filter; p, entrance slot; Q, photomultiplier; R, is iris tube.

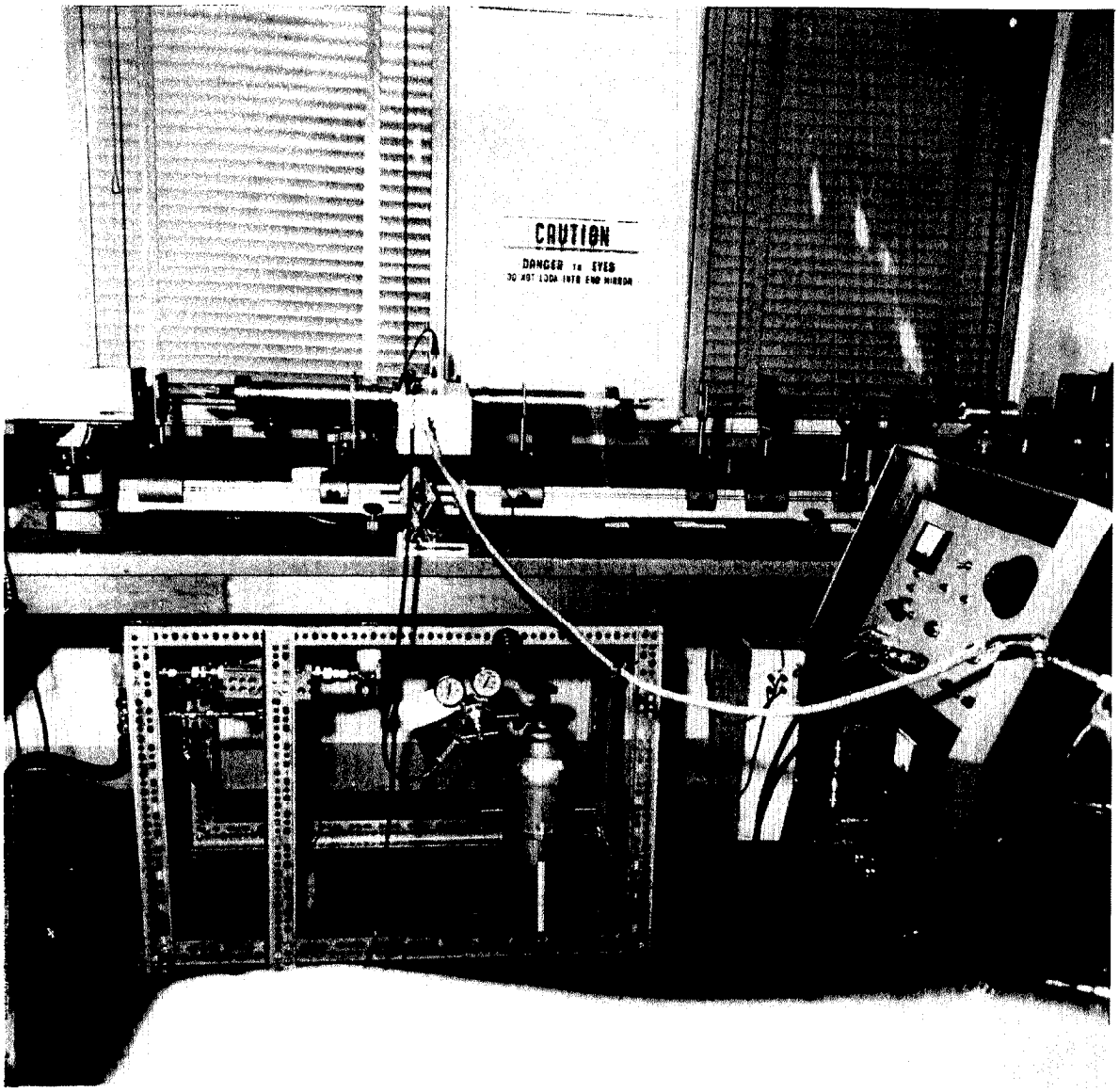


Figure III-5: General view of scattering experiment.

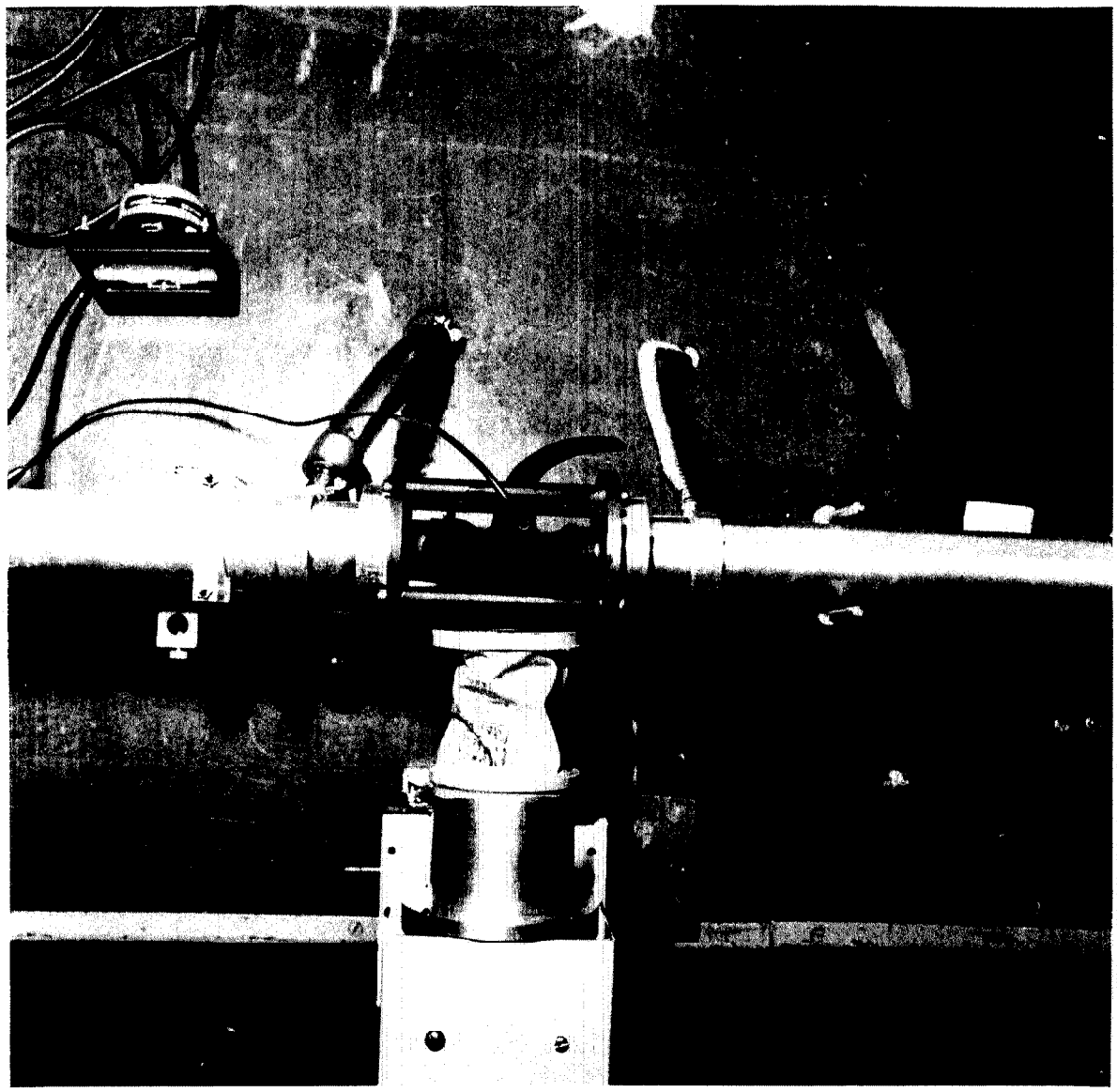

Figure III-6: Top view of scattering chamber.

of the laser power is found to get through the collimator.) It then passes through a Brewster-angle window made of quartz microscope slide (having indifferent flatness but low scattering) and through a tube containing eleven irises $\frac{1}{2}$" in diameter and 1.22" apart, whose inner circumferences are sharpened to a knife-edge. (The ratio of the length of the iris tube to its inner diameter has been found, in the course of building three separate models, to be an important parameter in the reduction of spurious reflections.) The light then passes through the scattering chamber through a second, identical, iris tube, and out of the vacuum chamber, where its relative intensity is measured by an I.T.T. FW-114A high-current biplanar photodiode.

The scattering chamber is equipped with a horn light trap of the kind mentioned by Lord Rayleigh. The horn is made of a blue cobalt glass having fair absorption in the red, cleaned carefully on the inside and coated on the outside with optical black paint. It provides a very black background to be "seen" by the detector; in Rayleigh's words, "a velvet cloth placed beside it appears a brilliant object." The aluminum electrodes are located in $\frac{1}{4}$" I.D. side tubes perpendicular to the scattering plane and are 4" apart. Scattered light emerging at $90^{\circ}$ to the incident beam is collected by a 2" lens and focused by another lens onto a horizontal slot about one mm high in front of the photocathode. On the way to the detector it passes through an interference filter equipped with a micrometer tilt adjustment, a corning 2-58 red filter, infra-red and visible blocking filters, and a vertical polarizer. The photodetector is an EMI 9558B photomultiplier. This tube has excellent

stability and sensitivity and low dark current, but was found to have a tendency toward saturation at moderate currents (see Appendix).

Much consideration was given to the problem of a good blacking with which to line the metal iris tubes. Most chemical blackings (such as ordinary anodizing) are actually good diffuse reflectors. Velvet is one of the blackest common materials but is obviously unsuitable to a vacuum system. Soot is a good blacking, but it was thought undesirable, as a possible source of loose particles which might cause scattering. Finally it was settled to use optical black paint. The thought of paint in a vacuum system is somewhat depressing; but it has been found that using a mechanical pump the vessel can be pumped down to the order of five microns. Even if the partial pressure of impurities is not decreased when helium is flowing through the vessel continuously, the impurity concentration will still be on the order of 0.1%, at which level it does not seem to interfere with scattering experiments. No paint is used on the walls of the glass scattering chamber. It seems probable that some chemical coatings as black as optical-black paint can be made, and if they do not absorb gases badly their use would represent an improvement.

The choice of the interference filter as the tunable element of the detector, in preference to a grating spectrometer, was made for several reasons. As will be shown in the next section, a suitable spectrometer must have straight slits, high dispersion, and a wide angle of acceptance; such an instrument would have to be specially constructed, which was not thought worthwhile until the feasibility of

the experiment had been established. Moreover if the detector has a narrow entrance slit, the laser light must be brought to a focus in front of the detector, as explained in section III-A. Not only does this make alignment difficult, but also the high fields resulting from focusing the laser might produce non-linear effects which would invalidate the results. The properties of interference filters are discussed in the next chapter.

Since the giant-pulse laser operates in a large number of modes it is, at any rate, difficult to reduce the beam radius $\rho$ to less than a few millimeters. Eq. III-2 then applies, the overall value of the quantity on the right being approximately $10^{-3}$ $n\sigma$.

D. Suggestions for Improvement of the Method

During the construction and use of the apparatus described above, several improvements and refinements have suggested themselves. The use of a gating and integrating circuit, in order to facilitate reduction of the detector bandpass, has already been mentioned in section III-B. Signal-to-noise ratios can also be improved by increasing the incident light intensity from the laser. This however, is a risky expedient, since various high-field effects are known to exist or are suspected of existing, and such effects might invalidate the measurements. (See Chapter II.)

The use of a grating spectrometer as the tunable element in the detector has been mentioned in section II-C. Such a modification would provide greatly improved resolution in spectral measurements.

However, in order to prevent inordinate loss of signal the spectrometer must have certain suitable properties. Firstly the optics should be designed in a manner which permits the use of a straight entrance slit (a curved exit slit may be used if necessary); for definiteness we shall assume that a Littrow mounting (in which the incident and diffracted beams make the same angle $\beta$ with the normal to the grating) is employed. Secondly it is important that the linear dispersion $\frac{dL}{d\lambda}$ be large, inasmuch as it is seen from Eqs. III-2 and III-3 that the entrance slit width $2w$ must not be small. The efficiency of the spectrometer must of course be as high as possible. Moderate overlapping of orders need not be a problem as the desired small wavelength region can be selected by means of a broad interference filter.

A well-known equation for the dispersion of a Littrow mounting is

$$\frac{dL}{d\lambda} = \frac{2P \tan \beta}{\lambda} \qquad \text{(III-44)}$$

P, the focal length of the instrument, is determined by the height $h$ of the grating through $h = 2P\alpha$, where as before $\alpha$ is the instruments half-angle of acceptance (Fig. III-1). In order to obtain larger dispersion we must employ a large value of $\tan \beta$. Because the groove aspect must be greater than the wavelength in order to obtain concentration of diffracted energy into the desired order, it is necessary that

$$\tan \beta < \frac{m}{2} \qquad \text{(III-45)}$$

where $m$ is the order of the diffraction maximum to be used. Since $\tan \beta$ is to be large we must work in a fairly high order. The grating equation

$$\frac{m\lambda}{a} = 2 \sin \beta \qquad \text{(III-46)}$$

provides a relation between the grating constant $a$ and the other parameters. The optimum blaze angle $\theta$ is obtained at $\theta = \beta$, and using Fraunhofer diffraction theory (valid when the groove aspect is much more than a wavelength) we obtain the following condition for a wavelength $\lambda$ to fall within the blaze:

$$\left|\frac{2\pi a}{\lambda} \cos \beta \left[\sin (\theta - \beta)\right]\right| < 1 \qquad \text{(III-47)}$$

The separation of the orders is obtained by differentiation of Eq. III-46:

$$\frac{d\lambda}{dm} = - \frac{2a \sin \beta}{m^2} \qquad \text{(III-48)}$$

The condition of working in a moderately high order suggests the use of an echelle-type grating. It will be easiest to use a grating which is available, and design around it. A replica ruled echelle of dimensions 4" by 8", having 270 grooves per mm and a blaze angle of $70^\circ$ is available from Bausch and Lomb. From Eq. III-46 we obtain $m = 10$. Simultaneous use of III-46 and III-47 gives that the blaze will be useful over a range 6500-7500Å, and that orders will be conveniently separated by 700Å. Using $\alpha = \frac{1}{9}$ as stipulated in section III-A we find

P = 45 cm, and from Eq. III-44 we find $(\frac{dL}{d\lambda})^{-1} = 29.5$ Å/cm. Since it is not practical to focus the giant pulse laser to a spot smaller than 3 mm with lenses of the necessary focal length, Eq. III-2 will apply and the limit for small $(\frac{bw}{c})$ can be employed:

$$\frac{P_s}{P_i} = n\sigma \frac{3R^2\ell}{8\pi^2\rho^2c^2} \left(\frac{dL}{d\lambda}\right)^2 (\Delta\lambda)^2 \qquad \text{(III-49)}$$

where $(\Delta\lambda)$ is the detector bandwidth (at the $\frac{1}{2}$-power points). If we settle upon $\Delta\lambda = 7$Å as for a good interference filter we find that

$$\frac{P_s}{P_i} = 7 \cdot 10^{-4} (n\sigma) \qquad \text{(III-50)}$$

The corresponding theoretical value of $P_s/P_i$ for the existing interference filter assembly (not realized because of losses in the filters and the fact that $\rho$ is not made as small as possible) is $2 \cdot 10^{-3}$ $n\sigma$. Thus the grating spectrometer receiver, if carefully designed, will be nearly as efficient as the interference filter.

In addition to the grating spectrometer, some other possibilities for tunable optical detectors exist. Since the amount of light from a diffuse source which can be put through any filter is roughly proportional to the square of the product of the angle of acceptance $(\alpha)$ and the aperture, it is desirable to maximize these quantities, provided it can be done without degradation of the bandwidth. One such device is the birefringent filter of Bernard Lyot.[III-14] This device can have bandwidth as small as a fraction of an Angstrom with apertures

of one inch or more. It can be tuned over a narrow range by changing its temperature (the coefficient for quartz elements being -0.66 Angstrom per degree Centigrade in the red), by rotating the polarizers, or by other means. Although the angle of acceptance of the filter in its simplest form is not great, various modifications have been suggested which attain angles of acceptance of more than half a radian. (The latter modification may not, unfortunately, be compatible with thermal tuning.) Lyot filters have been manufactured commercially by the German firm of Bernhard-Halle. An extensive study of the filter and some of its possible modifications are presented in a paper by T. W. Evans.[III-15]

The signal-to-noise ratio of the experiment could be improved if it were possible to perform it on a repetitive basis. Assuming that the noise is predominantly shot noise and not due to non-reproducibility, let us suppose we are interested in measuring a cathode current $i$ which repeats every $T_o$ seconds, and has duration $T$, thus having average value $\bar{i} = \frac{T}{T_o} i$. Superimposed on $i$ is the usual shot noise, but a gating circuit is used which removes the noise during times when $i$ is off. Then the average signal voltage across a parallel $rc$ filter having time constant $\theta$ long compared with $T_o$ is simply $\bar{i}r$. From energy considerations it is evident that the noise power is simply $(T/T_o)$ times its steady-state value:

$$\overline{(\Delta v)^2} = \frac{(2\pi)^{-1}\, e\epsilon g \bar{C}\bar{i}}{c^2} \int_{-\infty}^{\infty} \frac{d\omega}{\theta^{-2} + \omega^2}$$

$$= \frac{2e\epsilon g^2 C\bar{i}r}{c} \qquad \text{(III-51)}$$

The signal-to-noise ratio, again defined as the ratio of the expectation value of the measurement to its standard deviation, is then

$$R = \left(\frac{\epsilon \bar{i} \theta}{2eC}\right)^{\frac{1}{2}} \qquad \text{(III-52)}$$

Comparing with Eq. III-30 we see that the quotient of the R for the repetitive case by R for the case for single pulses is $(\theta/T_o)^{\frac{1}{2}}$. (Since $(\theta/T_o)$ is the number of signal pulses, III-52 is simply what is expected from the law of large numbers.) In the present state of the art $T_o$ can be of the order of one-tenth second, so that with quite reasonable integration times shot noise will cease to be a problem.

In addition to repetitive operation obtained by multiple operations of the laser flashlamp, it is also possible to produce a train of regularly spaced pulses from a single operation of the flashlamp. [III-16] Unfortunately the pulses obtained in this way until now have been approximately two orders of magnitude smaller than single giant pulses. However if sufficient signal level can be attained this technique could be very useful for plasma time development applications. Reliance on discharge reproducibility would then not be necessary.

As a final suggestion for possible future work, it has been

pointed out by many persons that photon-electron scattering experiments might be conveniently carried out in semiconductors. High densities of electrons should be easily attainable. So long as occupation numbers are kept low, and the electrons are in states having nearly constant effective mass, their behavior should not be different from that of free electrons, and one may expect that the interesting collective scattering effects predicted for dense plasmas would be observable. One possible obstacle is the scattering of the incident light by imperfections and thermal fluctuations in the crystal lattice. Lord Rayleigh [III-17] found that the scattering of light by a quartz crystal was eight times that of dust-free air, or equivalent to that of an electron density of the order of $5 \cdot 10^{16}$/cc (part of this scattering may be due to crystal imperfections); lattice scattering of this order should not present much difficulty. The theoretical problem of scattering from anisotropic crystals is complicated in general; a recent treatment is that of Duboc.[III-18] One would expect the lattice scattering to be least severe in materials with high Debye temperature, which if necessary could be refrigerated.

## REFERENCES


III-1. S. M. Berman, "Electromagnetic Radiation from an Ionized Hydrogen Plasma", Space Technology Laboratories Technical Report PRL 9-27 (24 Sept., 1959).

III-2. R. C. Rempel, "Optical Properties of Lasers as Compared to Conventional Radiators", Spectra-Physics Corp. Technical Bulletin No. 1, (June 1963).

III-3. H. Z. Cummins, N. Knable and Y. Yeh, Phys. Rev. Letters 12, 150-153 (Feb., 1964).

III-4. A. W. Hall and N. H. Williams, Physical Review 25, 147-173 (1925).

III-5. V. K. Zworykin, G. A. Morton and L. Malter, Proc. I.R.E. 24, 351-375 (March 1936).

III-6. K. R. Spangenberg, Vacuum Tubes, McGraw-Hill, New York (1948) pp.319-321.

III-7. W. Shockley and J. R. Pierce, Proc. I.R.E. 26, 321-328 (1938).

III-8. W. B. Davenport and W. L. Root, Random Signals and Noise, McGraw-Hill, New York (1958), p.144.

III-9. H. Bruining, Physics and Applications of Secondary Electron Emission, McGraw-Hill, New York (1954), p.115.

III-10. E. Funfer, B. Kronast and H-I Kunze Physics Letters 5, 125-7 (June 1963).

III-11. Lord Rayleigh, Proc. Roy. Soc. 97, 435-455, (1920).

III-12. T. V. George, L. Slama, M. Yokoyama and L. Goldstein Phys. Rev. Letters 11, 403-406 (Nov. 1, 1963).

III-13. E. Thompson and G. Fiocco, Bull. Am. Phys. Soc. 8, 372 (April 1963).

III-14. B. Lyot, Comptes Rendus 197, 1593-6 (1933).

III-15. T. W. Evans, Journal of the Optical Society of America 39, 229-242 (March 1949).

III-16. A. T. Ellis and M. E. Fourney, Proc. I.E.E.E. 51, 942-3 (June 1963); also A. Ellis, private communication.

III-17. Lord Rayleigh, Proc. Roy. Soc. 95, 479-487 (1919).

III-18. C. A. Duboc, Light Scattering from Single Crystals, Ph.D. Thesis in Physics, M.I.T., 1949.

# CHAPTER IV

## RESULTS OF SCATTERING EXPERIMENTS

The apparatus the design of which was considered in the previous chapter has been used to perform several experiments. The object of these experiments is to test the concepts that have been mentioned, establish the feasibility of the method, and determine its strengths or inadequacies as a diagnostic tool.

### A. Observation of Free-Electron Scattering

A typical arrangement of the triggering circuits is illustrated in Fig. IV-1. In order to obtain stability in the time of the laser pulse with respect to the initiation of the gas discharge, the oscilloscope trigger was obtained from the discharge current pulse itself. Since a certain amount of "hash" was present at the time of breakdown, a simple low-pass filter was inserted to give a triggering signal that represented the actual rise of the average discharge current. This resulted in laser timing that could be adjusted within an accuracy of 0.1 microsecond. The delay at which the laser pulse (approximately .05 microsecond in duration) was injected could be adjusted, using the oscilloscope auxiliary time base, between one microsecond and several hundred microseconds after initiation of the discharge. After the sweep of the oscilloscope (Tektronix 555 or 585) had been initiated, the sawtooth from the oscilloscope was used to trip the laser Kerr cell midway in the sweep.

The signal input to the oscilloscope was obtained from an E.M.I. type 9558-B photomultiplier. The output of this tube was passed through a short length of low-capacity RG-71 cable terminated in its characteristic impedance. Measurements made using a capacitive load were also tried; these were under some conditions rendered difficult by the integration of background plasma luminosity photocurrent, and so in general peak photocurrent measurements were used. The expectation that such measurements would not have substantially greater variance when made with the type 555 oscilloscope (rise time approximately .014 microsecond) was confirmed by comparison tests in which little, if any, difference could be detected. That large errors were not introduced by changes in the laser pulse waveform was indicated by the fact that the laser monitor, whose output was usually applied to the second trace of the oscilloscope, varied less than five per cent from shot to shot. This monitor was a high-frequency, high current planar photodiode, I.T.T. type FW-114A, whose transmission line was also terminated in its characteristic impedance.

The plasma itself was created by the discharge of a two-microsecond square pulse-forming network between cold aluminum electrodes, in series with a resistor of the network's characteristic impedance. Since the impedance of the discharge varies with current, the shape of the current pulse is degraded somewhat. Gas pressures are those measured using Hastings-Raydist VT-4 thermocouple gauge. The discharge current pulse for a discharge in helium at 6 mm is shown on the lower trace of Fig. IV-2. The upper trace shows the plasma luminosity of

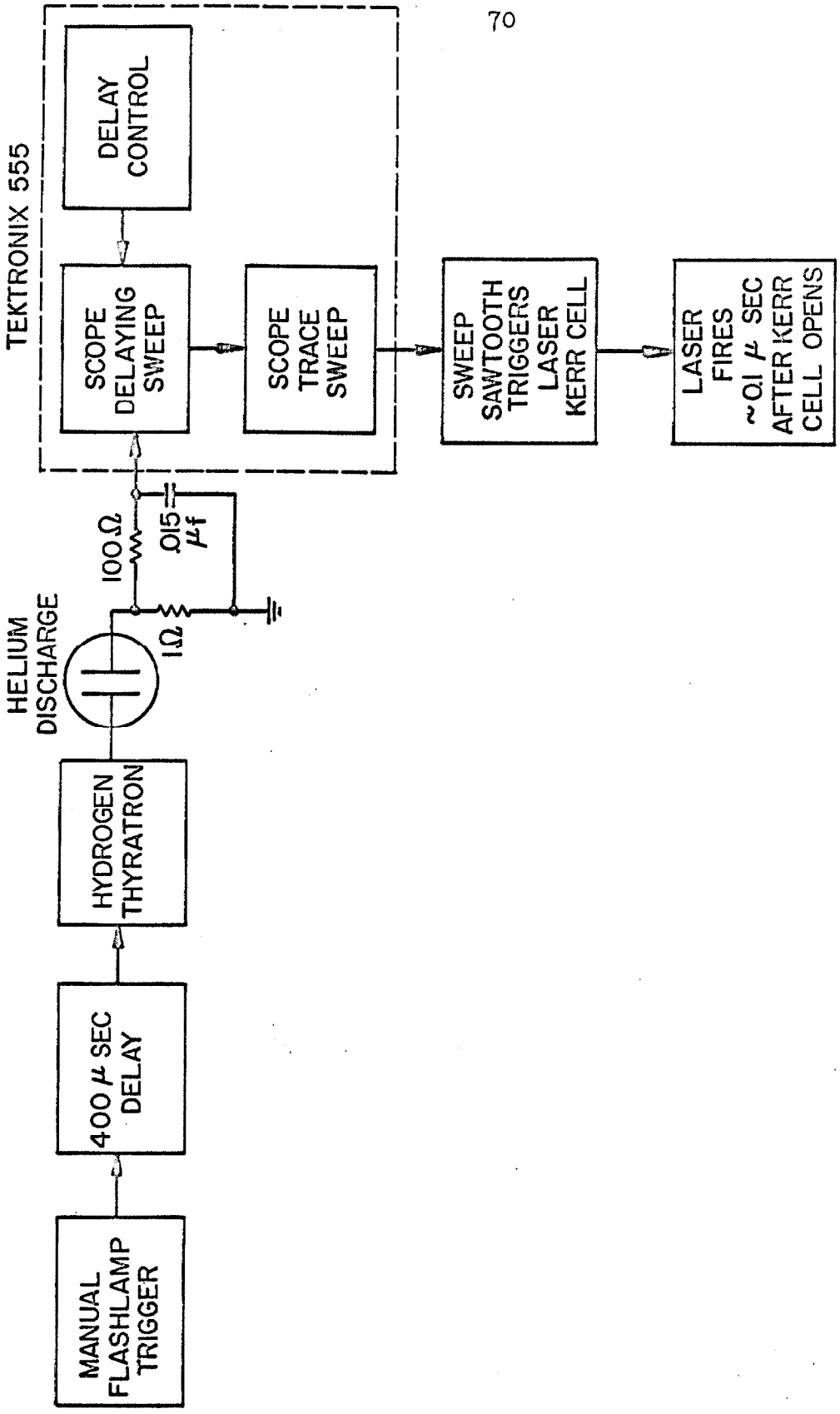


Figure IV-1: Block diagram of trigger circuits for afterglow scattering measurements.

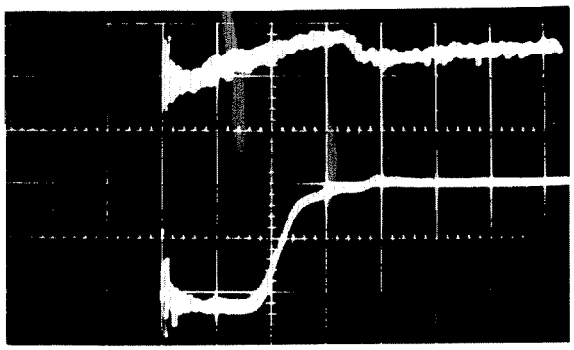

Figure IV-2: Upper trace: Luminosity of helium discharge at 6 mm. (Increased light reads downward.) Lower trace: Discharge current, 20 Amperes per division. (Increased current reads downward.) Time scale one microsecond per division.

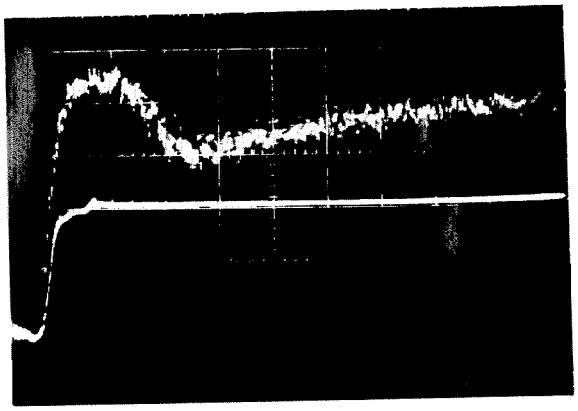

Figure IV-3: Upper trace: Luminosity of Argon discharge at 5 mm. (Increased light reads downward.) Lower trace: Discharge current, 20 Amperes per div. (Increased current reads downward.) Time scale two microseconds per division.

helium at $p = 6$ mm, as seen through the 6943Å interference filter and a vertical polarizer. Both traces were highly reproducible, at least to reading accuracies of five and ten per cent, respectively. The rise in the plasma luminosity just after the cessation of discharge current is thought to indicate the cooling of the plasma electrons, which results in an increased rate of recombination. Let us make an order-of-magnitude calculation of the electron cooling time, assuming that the electrons lose their energy by elastic collisions occurring with an average collision frequency $\nu$. Then if $\bar{\epsilon}$ is the average electron energy our rough calculation gives

$$d\bar{\epsilon} \simeq -\frac{2m}{M}\bar{\epsilon}\,\nu\,dt$$

$$\bar{\epsilon} \simeq \bar{\epsilon}_o\, e^{-\frac{2m}{M}\nu t} \qquad \text{(IV-1)}$$

where $M$ is the atomic mass. The order-of-magnitude cooling time is

$$t_c \simeq \frac{M}{2m\nu} \qquad \text{(IV-2)}$$

where $\nu$ is expected to be proportional to the gas pressure. If we insert $M/m = (4)(1836)$ for helium, and take $p = 6$ mm, $\nu = 6 \cdot 10^7$/sec, we get the order-of-magnitude result $t_c \simeq 0.5$ μsec. Fig. IV-3 shows the same quantities for a discharge in Argon at 5 mm. (Note that the time scale is not the same.) The local maximum in luminosity occurs later, presumably both because of the increased value of $M/m$ for argon and its low cross-section for inelastic collisions with electrons

with energy of two volts or less. Increasing the helium pressure also causes the luminosity maximum to occur earlier, as expected.

When the laser is fired into cold helium at 6 mm, no discharge being made, the result is as shown in Fig. IV-4. The result of firing the laser into the discharge at the time of the minimum of luminosity is shown in Fig. IV-5. The vertical magnification of the upper trace of Fig. IV-4 is twice that of Fig. IV-5. The very small signal received in the case of no discharge is due to wall reflections (the Rayleigh scattering from the helium is very much smaller); the oscillations following the signal are pickup from the laser Kerr cell. In both figures the upper trace is delayed with respect to the lower. Careful comparison measurements between light scattered from the discharge and intentionally increased wall reflections indicate that the time of arrival of the plasma scattered light and the incident laser pulse do not differ by more than .01 microsecond. Note also in Fig. IV-5 that the shapes of the incident and scattered pulses are similar, in that the rise of the pulse is more abrupt than the fall; this shape agrees with published theories of laser behavior.[IV-1]

A Polaroid Type HN-32 polarizer (described in the previous chapter) was in place before the scattered light detector, oriented to transmit light having its E-vector perpendicular to the scattering plane. When this polarizer was rotated $90^{\circ}$, less than 10% of the former signal was received. This is in agreement with the theory of Thomson scattering which indicates that if the incident light is completely polarized, the scattered light should be completely polarized.

As the shutter of the giant-pulse laser, both a nitrobenzene Kerr cell and a solid-state potassium dihydrogen phosphate (KDP) cell were employed at various times (see Appendix). The nitrobenzene Kerr cell is known to introduce into the laser output a component of infrared radiation at 7660Å, through stimulated Raman scattering.[IV-2] When the Kerr cell was in use a dielectric-layer infrared blocking filter was used to exclude this radiation. When the KDP cell was in use, and the incident light presumably was purely at 6943Å, the blocking filter was inserted and removed. The change in signal level was equal to the small transmission loss of the filter at 6943Å. This indicates that no infrared radiation produced in the plasma-laser interaction had an influence on the measurements.

As a test to assure that a non-linear process of some kind was not taking place, a sequence of measurements was made, varying the laser peak power and holding other conditions constant. Laser powers were produced in the range one-half power to full power by varying the pumping energy and ruby temperature. The points were taken using a helium discharge at 6 mm, at 1.65 microseconds after the start of the discharge, with the interference filter at normal incidence. The results are shown in Fig. IV-6, and seem to lie reasonably well on a line through the origin.

A calibration of the scattered signal was obtained by filling the scattering chamber with a gas whose Rayleigh scattering cross-section is known. Using argon, the ratio of the Rayleigh scattered intensities from the gas at .95 mm and 1.9 mm, averaged over two shots

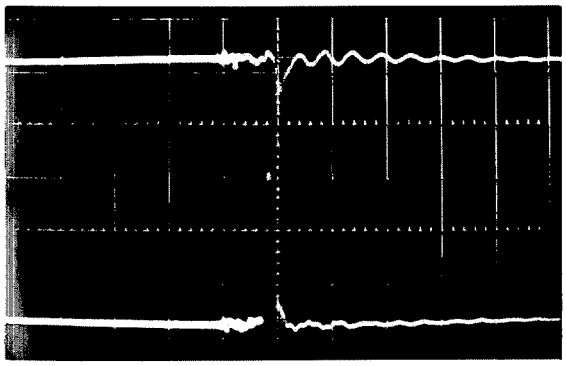

Figure IV-4: Upper trace: Received signal when no plasma is present. (Increased light reads downwards.) 0.5 mA phototube current per division. Lower trace: Laser monitor. Traces are not synchronized. Time scale 0.2 microsecond per division.

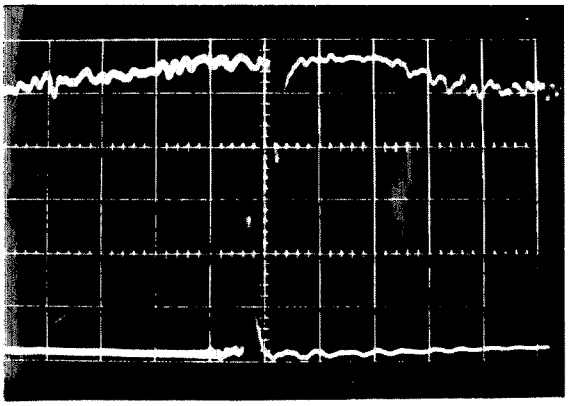

Figure IV-5: Upper trace: Received signal when plasma is present. (Increased light reads downwards.) 1.0 mA phototube current per division. (Note that scale is one-half that of Fig. II-4.) Lower trace: Laser monitor. Traces are not synchronized. Time scale 0.2 microsecond per division.

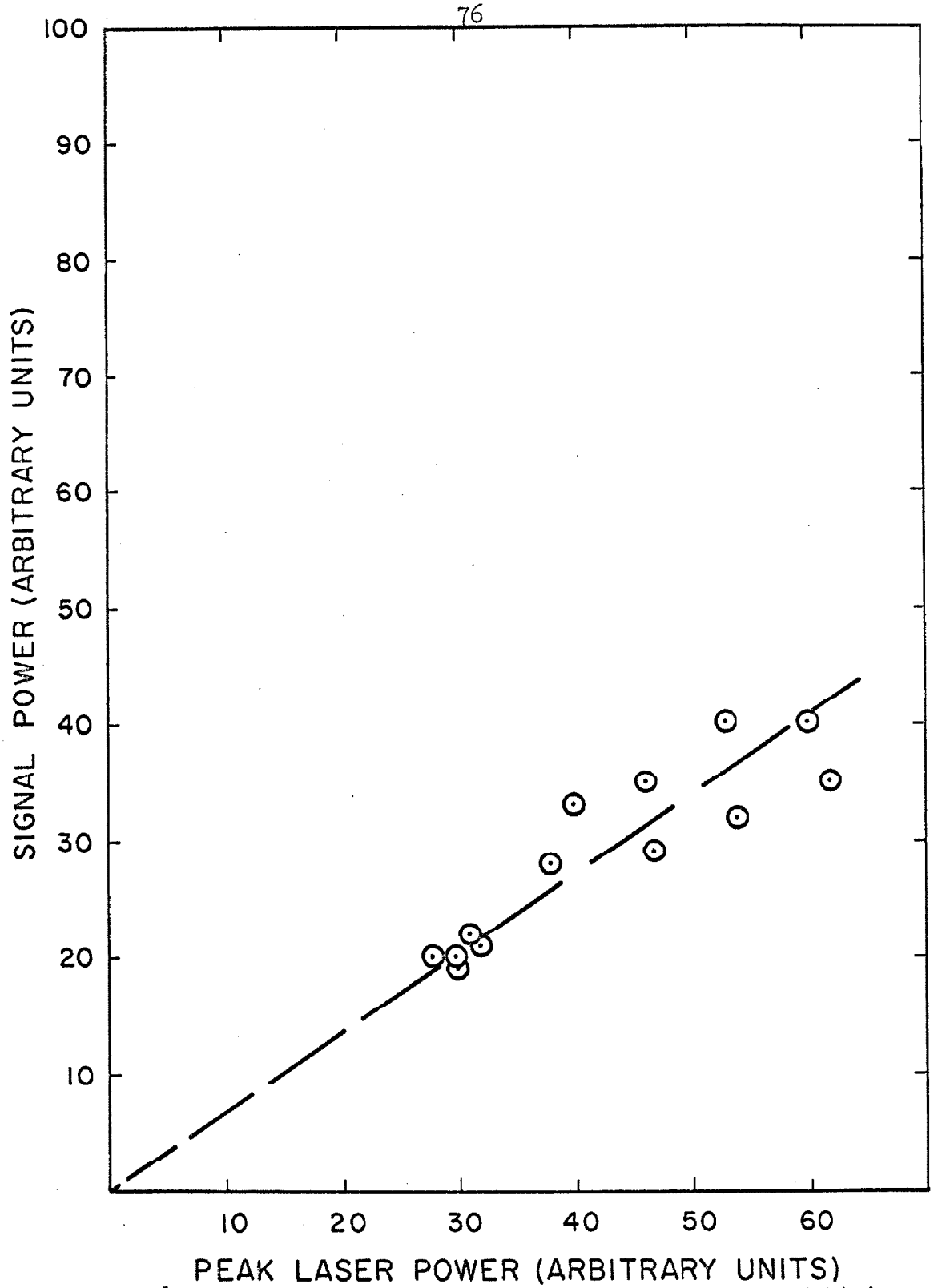


Figure IV-6: Intensity of scattered light versus incident light intensity. Time 1.65 μsec after cessation of current; Helium discharge of 6 mm pressure; filter at normal incidence.

apiece, was 1.88, the difference from 2.00 being within the random errors (assuming the ratio of pressures is given correctly by the thermocouple gauge). Scattering from nitrogen and air (which have nearly the same calculated cross-sections) were of the same order of magnitude. Scattering from helium at atmospheric pressure indicated a cross-section two orders of magnitude smaller; the calculated cross-section of helium is 1/70 that of argon. Using the argon scattering, it was found that the electron density in the helium discharge at a time eighteen microseconds after cessation of the current was $8.85 \cdot 10^{13}$ electrons per cubic centimeter. This is in good order-of-magnitude agreement with the estimate of density obtained using the magnitude of the photocurrent, the apparatus geometry according to Eq. III-2, and estimated photomultiplier sensitivity.

In order to observe the random velocities of the free electrons experiments designed to detect Doppler broadening of the returned light were carried out. The method was that of tilting the interference filter of the detector by means of a micrometer screw. When tilted, the center frequency of the filter moves toward shorter wavelengths, the peak transmission decreases, and the passband widens. Fig. IV-7 shows the approximate transmission curves of the filter for various tilt angles, designated on the figure by the number of turns of the micrometer screw (henceforth simply called "turns"). These curves were obtained by using a Jarrell-Ash $\frac{1}{2}$-meter monochromator as tunable light source, with an optical configuration designed to simulate as closely as possible the configuration of the scattering chamber. However, the

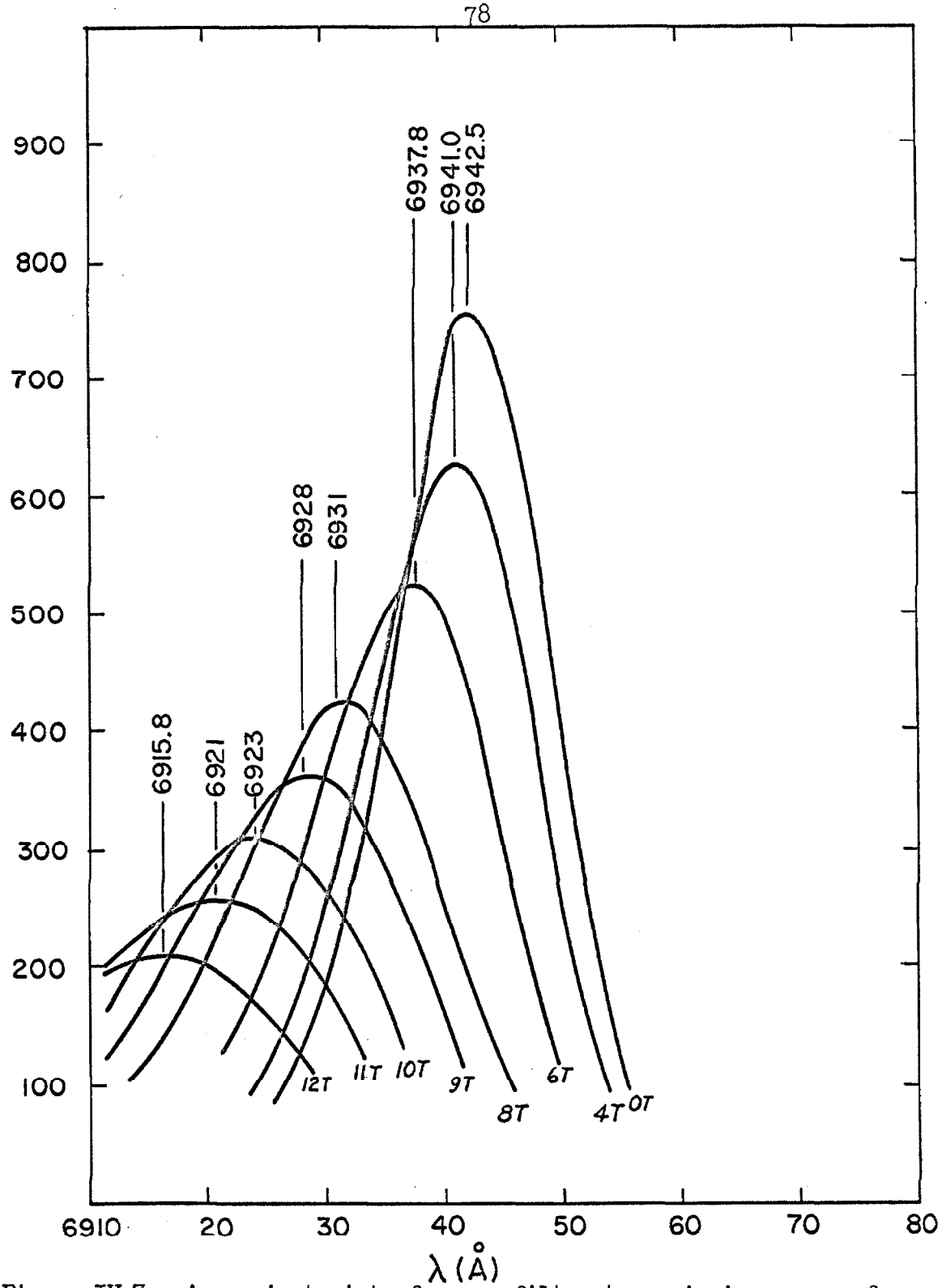


Figure IV-7: Approximate interference filter transmission curves for various tilt angles, designated by number of turns of micrometer screw. Figures above curves are wavelengths of maximum transmission. Data from monochromator measurements. Vertical scale in arbitrary units.

filter is highly sensitive to the angular distribution of the light passing through it, and so for actual determination of Doppler broadening it is safer to determine its transmission characteristic under the actual conditions of the experiment. This is done by filling the chamber with a gas which is an efficient Rayleigh scatterer, and plotting the power of this presumably monochromatic scattered light as a function of turns. Such a skirt transmission curve, obtained from scattering by air at a pressure of one millimeter, is shown in Fig. IV-8. It should be noted that because the transmission characteristics become lower and wider as the filter is tilted, the area beneath the filter curve stays approximately constant. A curve of the product of peak transmission and width at half-transmission point, obtained from Fig. IV-7, is shown in Fig. IV-9. This is approximately the curve which would be obtained if the scattered light were "white". It is to be expected that if the light scattered by the plasma is somewhat broadened, a curve somewhere intermediate, between the curves of Figs. IV-8 and IV-9, will be obtained.

Two graphs showing the plasma scattering data presented in this way are shown in Figs. IV-10 and IV-11. The former set of data was taken at a time 2.2 microseconds after the start of the discharge (which occupies roughly the time zero to two microseconds); the latter at 3.0 microseconds. The scatter of experimental points is greater in Fig. IV-10 than in IV-11 because each point on the former represents a single laser shot, while in the latter each plotted point is the average of three shots. In Fig. IV-12, these curves are again shown, together

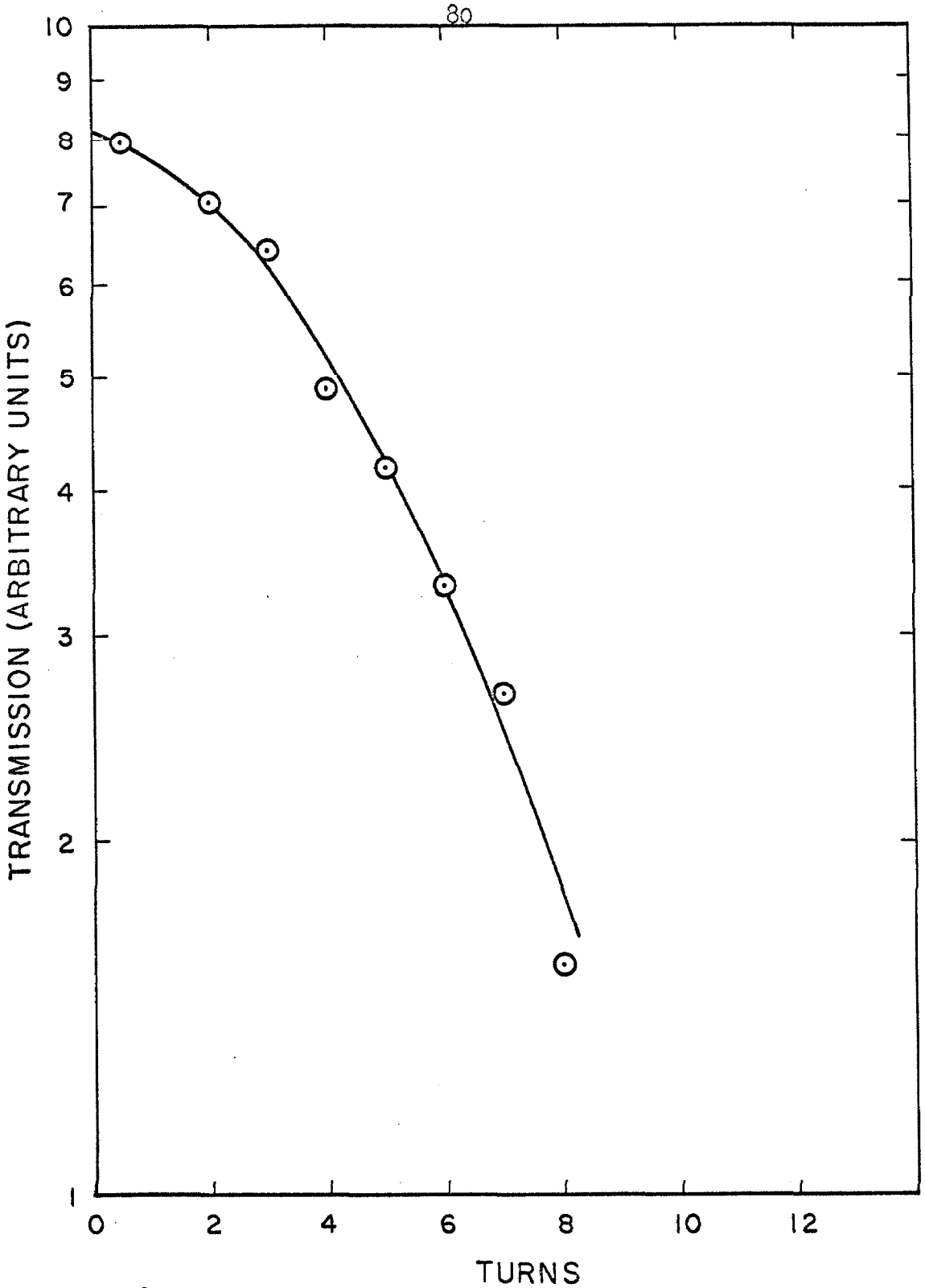


Figure IV-8: Experimental transmission curve of interference filter for monochromatic 6943A light, as a function of turns of micrometer screw. (Solid line.) Scattering data from air at 1 mm pressure.

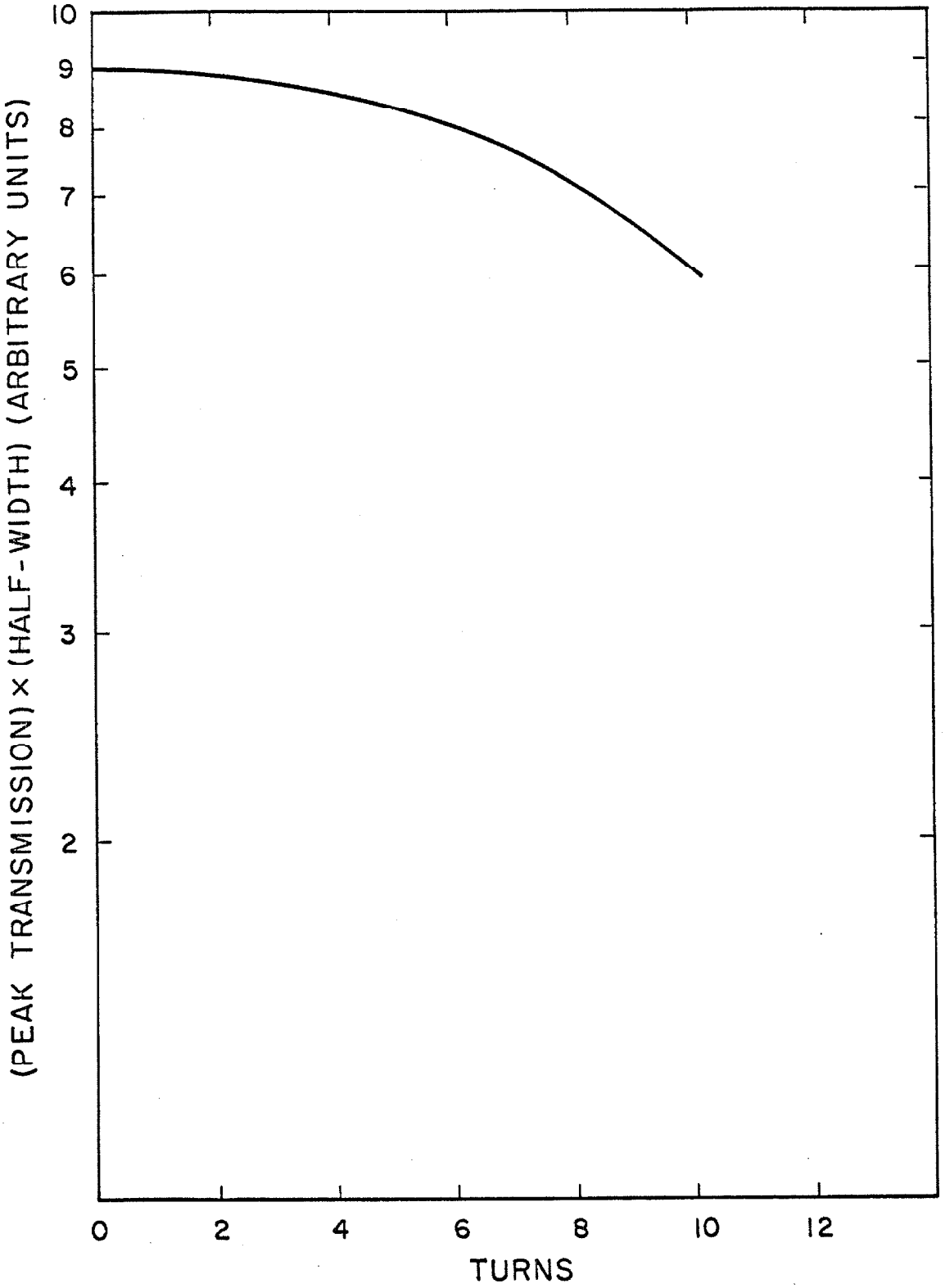


Figure IV-9: Product of peak transmission and width at half-transmission as a function of tilt angle, from Fig. IV-6.

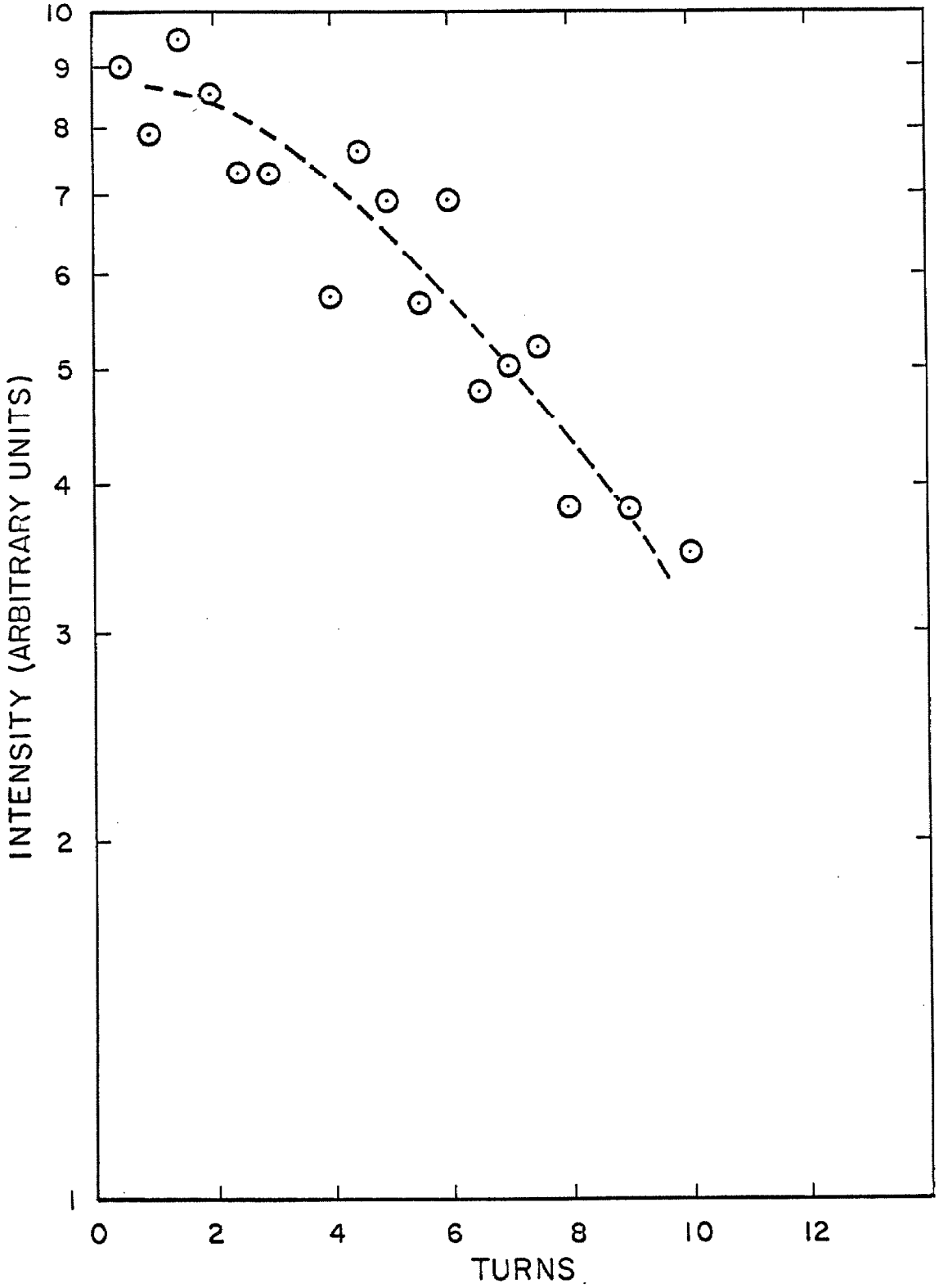


Figure IV-10: Intensity of plasma-scattered light versus angle of interference filter; T = 2.2 μsec.

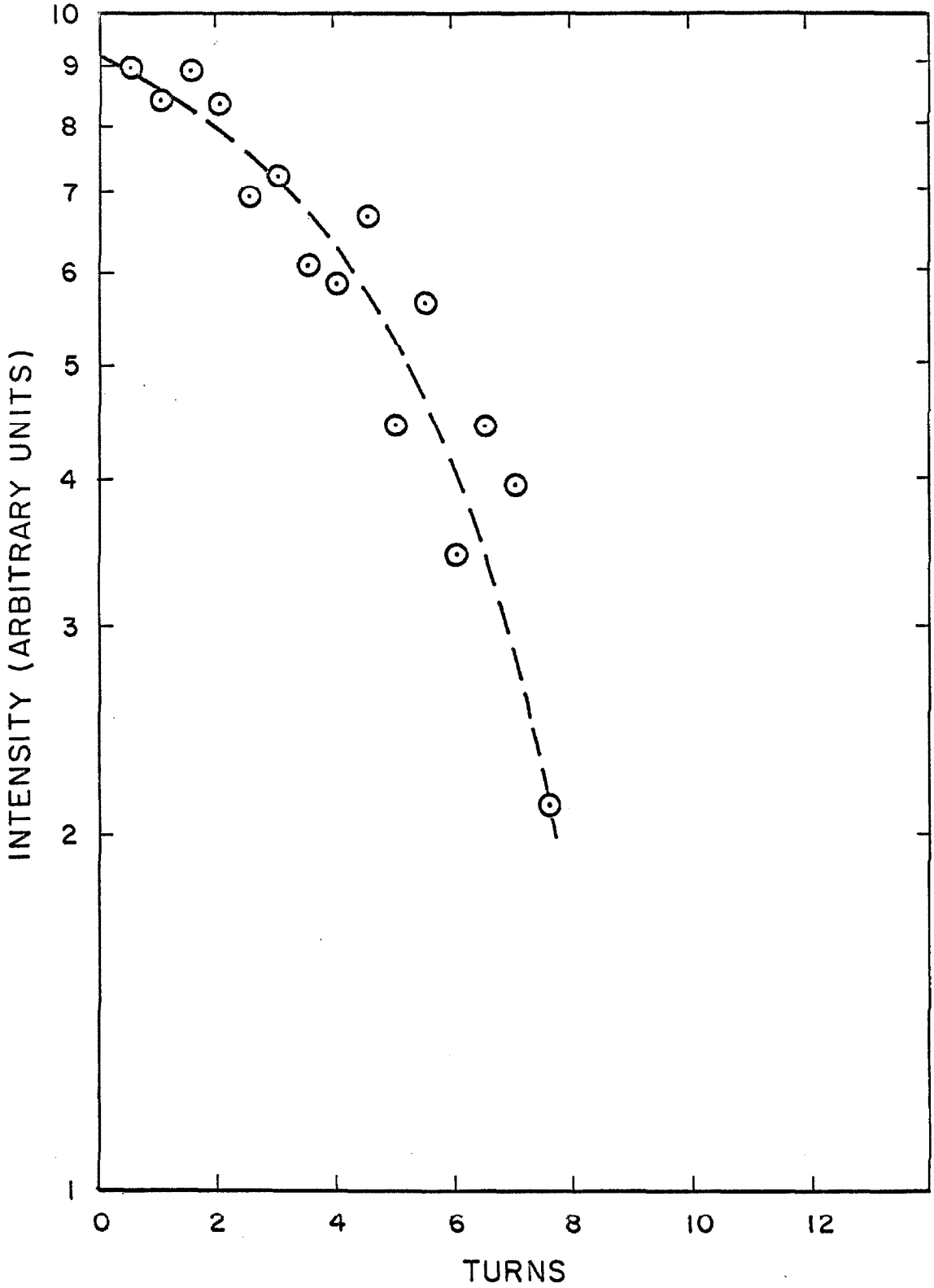


Figure IV-11: Intensity of plasma-scattered light versus angle of interference filter; T = 3.0 μsec.

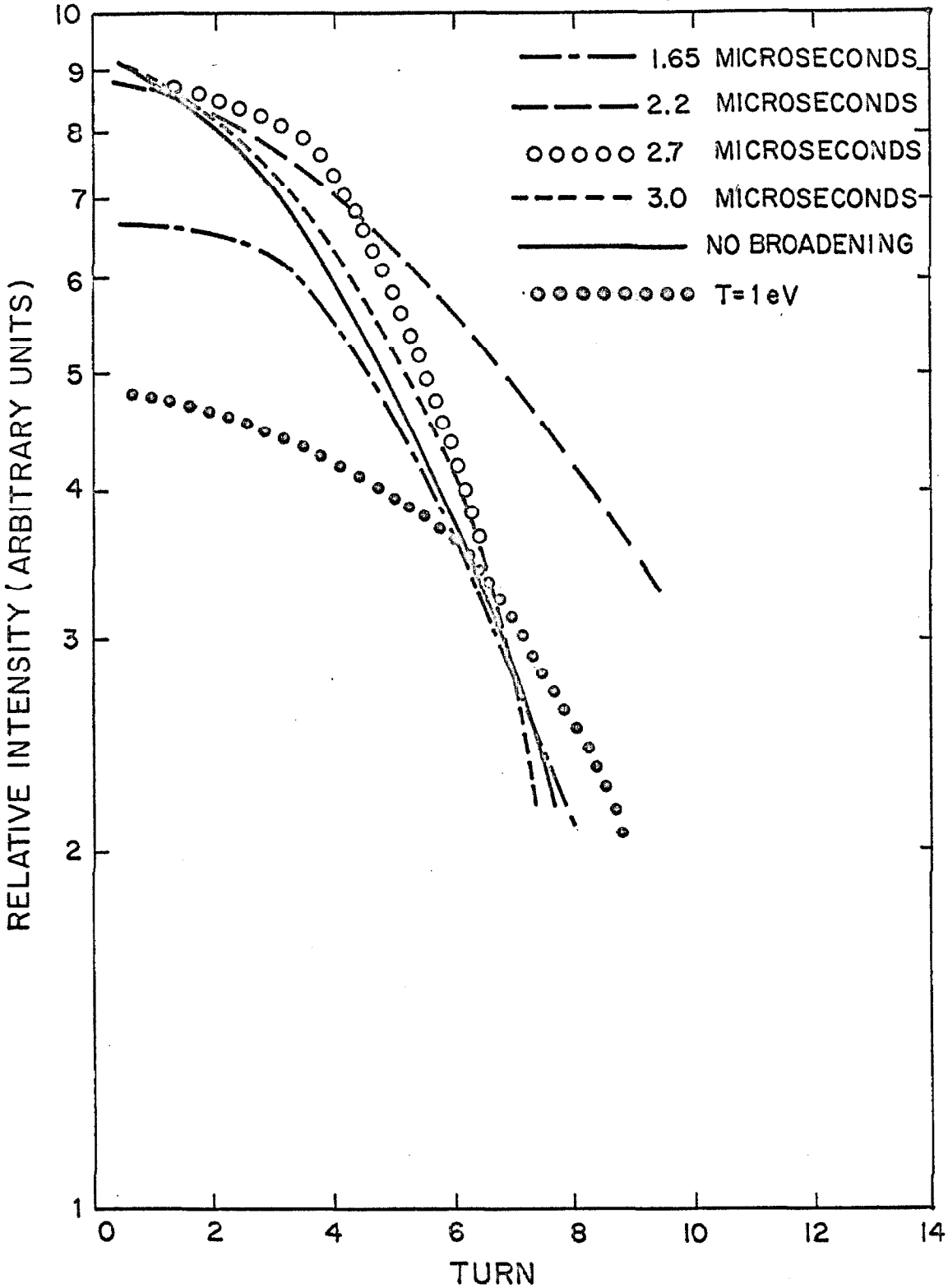


Figure IV-12: Intensity profiles for scattering at various times. Expected profiles for no broadening, and for an electron temperature of one eV are also shown.

with others at 1.65 μsec and 2.7 μsec. The scattering curves are shown to scale with one another; i.e. the respective intensities are indicated by the figure. Also shown on this figure are the experimental skirt transmission curve for monochromatic light, Fig. IV-8, and an approximate curve calculated from the data of Fig. IV-7, indicating the expected shape of the scattered light profile, assuming a plasma described by an electron temperature of one eV and an electron density the same as the final density taken from the 3.0 microsecond curve.

The curve taken at 1.65 μsec was made at a time when the discharge current was still on. It indicates a scarcity of slow electrons, as one might expect; presumably many electrons have such high velocities that their scattering is beyond the transmission region of the filter. The 2.2 μsec curve shows an increase in the number of both slow and faster electrons. The curve at 2.7 μsec shows a further increase in slow electrons, but a decrease in the number of faster electrons. The curve at 3.0 microseconds has almost exactly the shape expected for "cold" electrons.

The curve for 2.2 microseconds has a shape similar to that expected for a temperature of 1 eV. An interesting feature of this curve is its high relative amplitude; if the total number of electrons were constant, its amplitude should be that shown for the theoretical 1 eV curve. Possibly this can be explained by the observation that the faster electrons are more likely to be lost through diffusion than the slower, so that the former are removed. Using the reported value of the ambipolar diffusion constant in helium (560 $cm^2$/sec at 1 mm Hg,

$300^{\circ}$ K, [IV-3] and if we assume that this constant is proportional to the electron temperature, that the ionization is initially contained in a region whose characteristic dimension is on the order of one-half centimeter, and that first-mode diffusion takes place, then we find that electrons at a temperature of 3 eV are lost with a characteristic time on the order of one microsecond. (When the electrons have been cooled to room temperature the diffusion time is on the order of one millisecond and hence diffusion is unimportant.) Thus it seems reasonable that the number of slow electrons remain relatively constant, while the energetic electrons are removed by their motion from the region of interest.

The technique of the tilted interference filter is rather unsuited to the precise measurement of electron velocity distributions; it is a very coarse resolving technique, in which different distributions might give similar results. This work will be carried out to better advantage when a spectrograph is used as the tunable detector. However the data of Fig. IV-12 definitely indicates broadening of the scattered light for times earlier than three microseconds, and thus makes it seem very probable that the scattering is by free electrons.

## B. Application to Afterglow Studies

A unique capability of the apparatus described in the preceding chapter is that of making scattered-light density measurements on "cold" plasmas; that is, without reliance on Doppler broadening. This capability makes it particularly suitable to afterglow measurements.

Although the purity of the discharge which has been described is unknown, and is possibly not high enough to yield physically meaningful information on afterglow processes, it has been thought worthwhile to perform afterglow scattering measurements upon it, for the purpose of demonstrating the feasibility or shortcomings of the technique.

It is assumed that for a cold plasma in which the parameter $\alpha = (k\lambda_D)^{-1}$ is small compared to unity (notation is that of Chapter II), the intensity of the scattered light is directly proportional to the number of electron scatterers in the detector's field of acceptance. The laser is triggered at various times after cessation of the discharge current, and the peak energy of the scattered light recorded. The peak intensity of the incident light is registered by the biplanar photodiode monitor, and the quotient is then proportional to the number of scatterers. The experimental arrangement is similar to that described above, except that the interference filter in the detector is permanently set to normal incidence. The jitter in the time of laser triggering, as has been mentioned, is of the order of 0.1 microsecond.

The result of such a set of measurements is shown in Fig. IV-13. A curve was passed through these points freehand and, after correction for collective effects according to Eq. II-14, is shown again on Fig. IV-14.

Also shown in Fig. IV-14 are the intensities of three spectral lines of helium and the intensity of the hydrogen $\beta$ line (4861Å) in the afterglow. The relative intensities of the spectral lines are not indicated in the figure; in particular the maximum intensity of $H\beta$

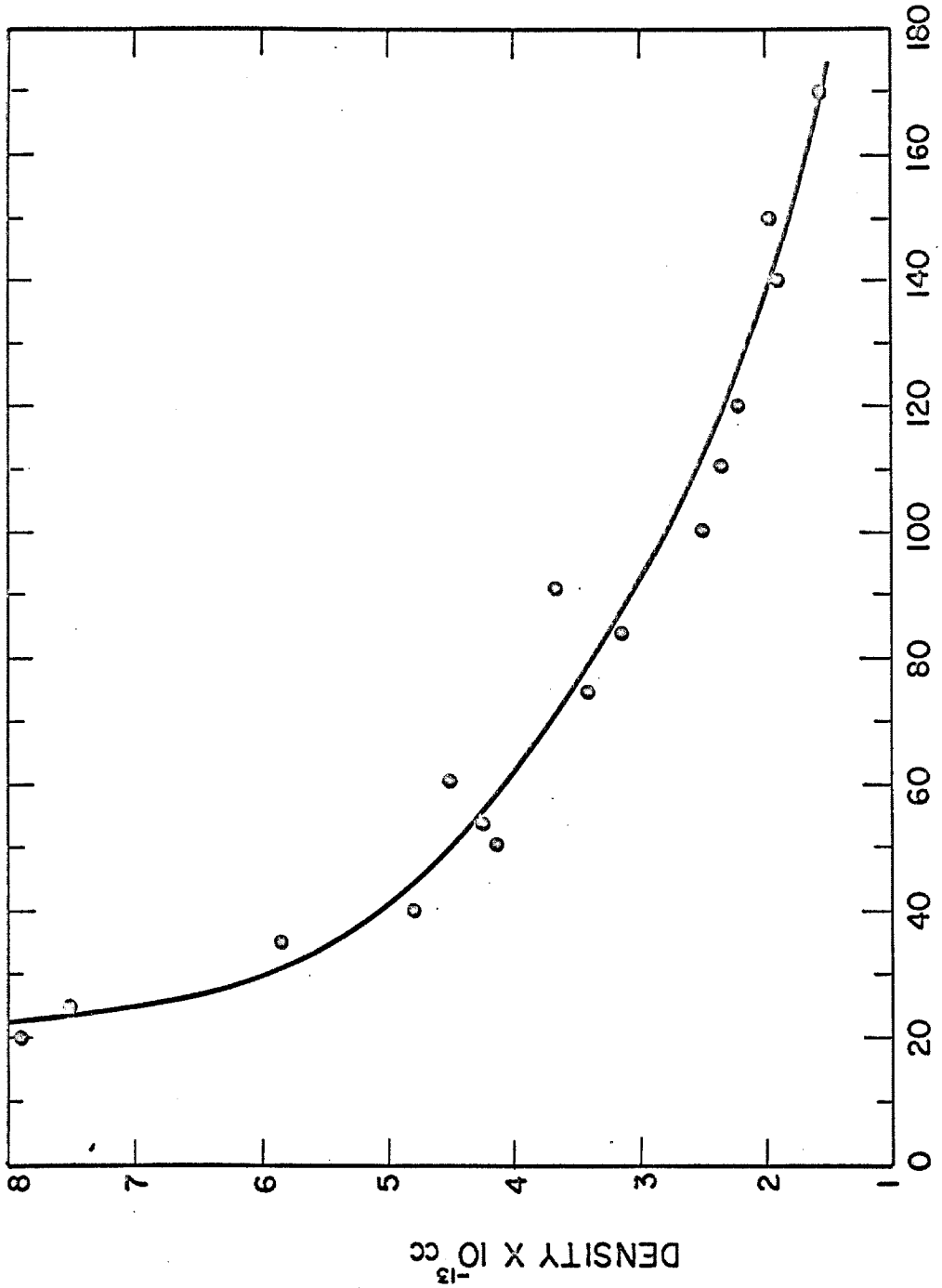


Figure IV-13: Electron density versus time from scattering measurements.

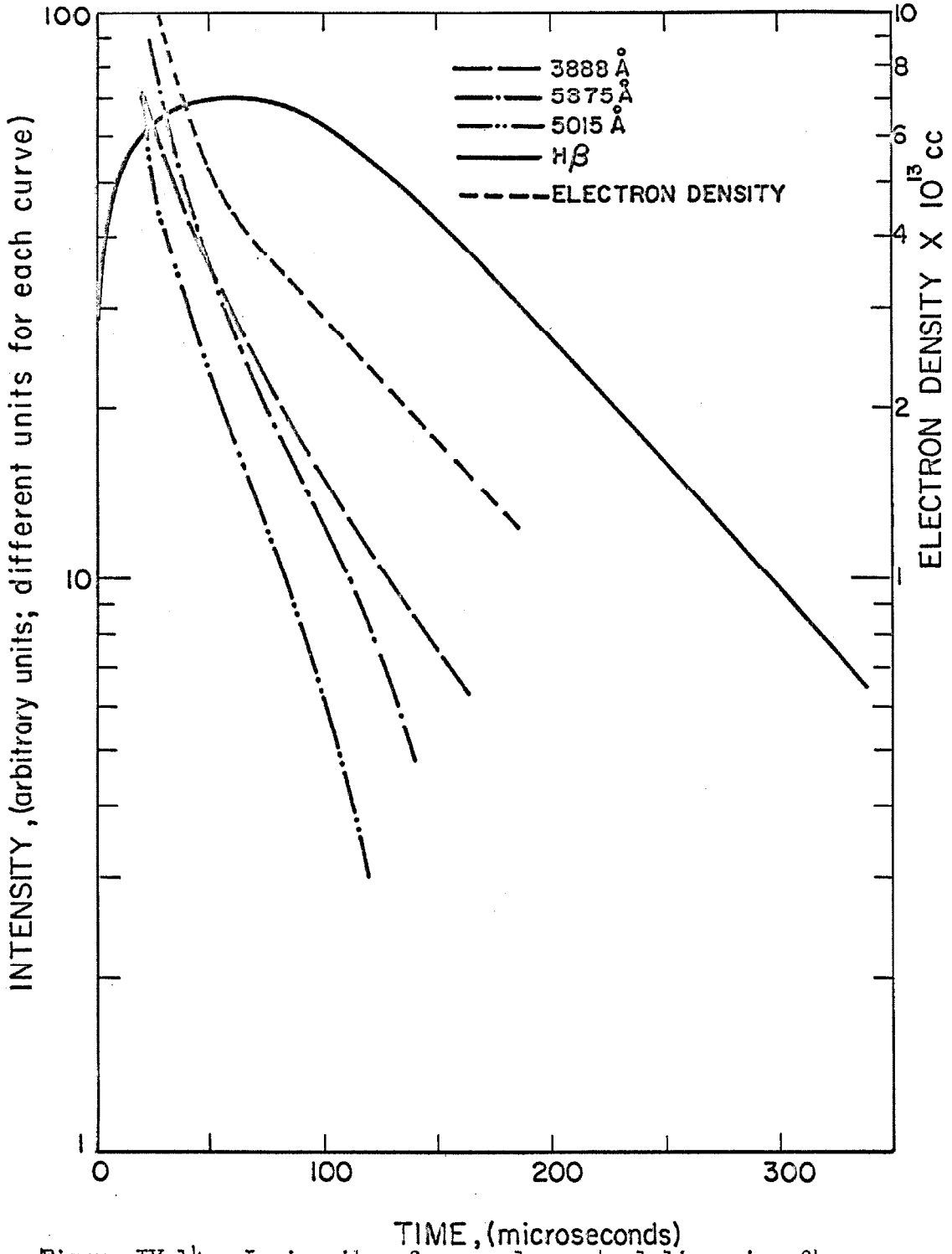


Figure IV-14: Luminosity of several spectral lines in afterglow. (The relative intensities of the lines with respect to one another is not indicated by the figure.) Density curve from scattering measurements is also shown.

is about 10% of the intensity of the strongest helium line, at 5875Å, at the same time. No lines of any other element were found, although numerous very weak molecular lines are present. Diffusion should not be an important process in this afterglow, according to the published value of the diffusion constant in helium.[IV-3] This expectation is confirmed by the observation that curves of luminosity change very little with gas pressure. Nor should attachment be of great importance, as low-energy attachment cross-sections for typical impurity molecules are thought to be in the neighborhood of $10^{-20}$ $cm^2$.[IV-4] Nonetheless it appears that impurities do play a significant part in the behavior of the plasma, since hydrogen is somehow produced. Originally it was thought that the shape of the hydrogen luminosity curve indicated production of hydrogen in the afterglow; after the apparatus was taken down the thought occurred that it might have been due to Stark broadening of the line beyond the 1.5Å width of the slits. Computations suggest that the electron density indicated by the scattering measurements would not be enough to account for the luminosity curve, although a density on the order of twice as large might be sufficient. This point is being investigated further.

It is tempting to try to piece together a theory relating the behavior of the various curves of Fig. IV-14. However, the processes of the helium afterglow are poorly understood even for pure gases, with no theory of recombination being firmly established. Considering the additional uncertainty posed by the presence of impurities, any such theory would be only conjectural and so has been omitted here. The

electron density curve which has been obtained appears reasonable, and serves to indicate the manner of data which can be obtained.

## C. Discussion of Diagnostic Measurements

One evident defect in the data which has been obtained is the scatter of the points. The sets of data shown above are among the best which were obtained. Typically the ratio of average value to standard deviation was between five and ten, and of the order expected for shot noise according to the results of the previous chapter. Occasionally the scatter was worse, and this presumably was due to some unknown effect which caused the reproducibility of the discharge to deteriorate. If the discharge being diagnosed is highly reproducible, then the scatter of the points should not be a great limitation, since it can be reduced according to the suggestions made in Chapter III.

The range of densities which can be measured by the present apparatus lies above $10^{13}$ electrons per cubic centimeter. This is a highly useful feature, inasmuch as conventional microwave measurements become difficult at densities above $10^{13}$/cc, while the principal technique for dense plasmas, that of Stark broadening of hydrogen lines, is useful principally above $10^{15}$/cc. Thus the Thomson scattering method fills a "hole" in the range of plasma densities which can be measured. The restriction that the density be above $10^{13}$/cc is however, inconvenient for afterglow measurements, in which it is desirable to observe the density over many decades. The lower limit is set by the spurious wall reflections, and with sufficient ingenuity it can be improved upon.

It should also be noted that the scattering method is suitable to many diagnostic situations that are difficult or impossible by conventional techniques. When the time variation of the plasma is rapid, when its geometry is inconvenient, when the density is high (particularly if the ions are not hydrogen), or when measurement must be made at a specific point, rather than over a volume, and without disturbing the plasma: these are situations in which the trouble of making Thomson scattering measurements may be worthwhile. In particular, the plasma which has been used in these experiments would be very difficult to diagnose by any other means.

One additional, and rather peculiar, deficiency in the technique for afterglow measurements should be mentioned. It has been found that measurements beyond 50 microseconds into the afterglow are troubled with very large spurious scatterings. Because they are not ordinarily seen earlier than this, it has been thought that they are due to the presence of particles which have been accelerated by high fields at the electrodes. At times later than 180 microseconds the probability that such a scattering will take place begins to approach unity, and measurements become impossible. On the other hand it is possible that the cause of these spurious scatterings is more subtle, and perhaps related to the phenomena of the following section.

## D. Other Laser-Plasma Interactions

While making the measurements described above, two unexpected phenomena were observed. The first was the observation that sometimes

(15a)

(15b)

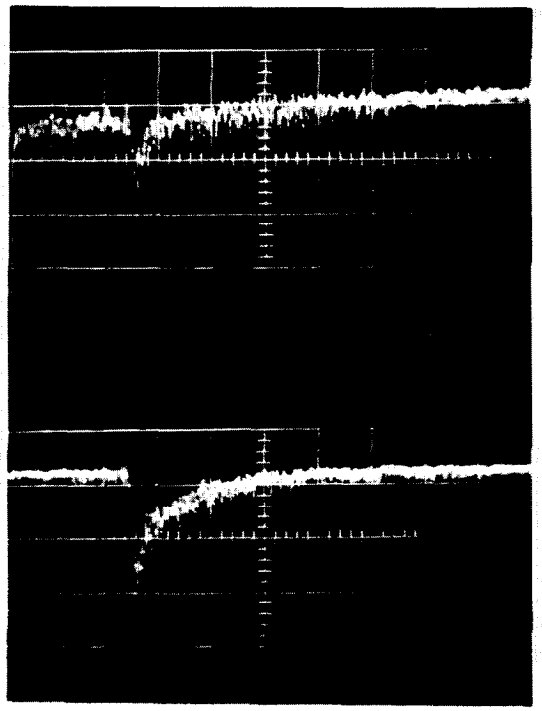

Figure IV-15: "Induced plasma luminosity" due to fifty-nanosecond light pulse. In Fig. 15a the laser was fired five microseconds after cessation of discharge current; in 15b, fifty microseconds after. Scale, two microseconds per division.

after the pulse of scattered radiation the plasma luminosity did not drop back to its previous value, but remained elevated, only gradually subsiding back to normal with a decay time of from one to two microseconds.(see Fig. IV-15) The second consisted in the observation of occasional "giant" scatterings several orders of magnitude greater than the normal electron scattering. The two phenomena, which have been mentioned previously in a preliminary report,[IV-5] will now be described.

Both phenomena occur only when the laser is fired into the discharge, and not when it is fired into the cold gas. Both seem to be related to the presence of certain impurities. As has been noted, the chamber in which the discharge is formed has on some of its interior surfaces (far removed from the discharge region) a coating of black paint which was applied in the process of reducing the wall reflections. In normal operation the chamber is being pumped continuously, and a constant flow of helium is kept passing through it, so as to keep the concentration of volatile impurities down to less than an estimated 0.1%. The phenomena do not occur under these conditions. However, if the pump and helium leak are valved off and impurities allowed to collect, then the induced luminosity begins to be noticed at an impurity concentration of around 0.3% and increases with the impurity concentration thereafter. Various controlled impurities have been introduced into the flowing helium in order to try to reproduce the phenomenon. Concentrations of more than 2% nitrogen, oxygen, hydrogen, and argon failed to produce the effect; however, a concentration of 1.5% propane

(itself containing a 4% butane impurity and perhaps traces of water or other material) produced an effect which seemed identical to that produced by the accumulated paint vapor. However the propane apparently is less effective, as the required concentration is greater. When the body gas into which the impurities are introduced is changed from helium to argon, the effect is still observed but is not so pronounced.

The induced luminosity is always more pronounced when the laser is fired into late afterglow than into the early afterglow, and decays more slowly (Fig. IV-15). The effect does not seem to decrease in magnitude when the laser power is decreased to half, indicating a surplus of available photons. The spectrum of the induced luminosity is not broadband, but centered either at the laser wavelength or at a longer wavelength (because the photodetector is tuned by tilting the 6943Å interference filter, it has not been possible to tune to longer wavelengths). It does not seem to be broadened significantly into the region of wavelengths less than 6943Å. When the discharge is observed through a 5460Å interference filter the effect cannot be seen. This seems to eliminate the possibility that the induced luminosity arises from a sudden increase in the electron concentration.

A similar phenomenon has been reported by Rose, Lidsky and Thompson;[IV-6] however, there are significant differences. In the observations of these workers a long ($\approx$ 1 millisecond) pulse of light from a normal laser was used, rather than a short ($\approx$ .05 microsecond) giant pulse; the enhanced radiation persists milliseconds after the laser light instead of microseconds, and the enhanced radiation is reported to be broadband.

The giant scattering phenomenon seems also to be related to the impurities in that it is more often seen when more of the latter are present. Unlike the induced luminosity, however, it is not observed reliably; sometimes it is present, sometimes not. As mentioned in the previous section even when no impurities are deliberately introduced, giant scatterings are sometimes seen. Because they are never seen earlier than approximately fifty microseconds into the afterglow unless impurities are added, they have been thought to be due to scattering from small particles emitted from the electrodes. However, it is possible that the two effects are the same.

A hypothesis which seems to agree with observation is that there is, in hydrocarbon molecules, a pair of excited states separated by the laser photon energy. When a burst of some $10^{18}$ photons is applied, the populations of the two states become equalized, then decaying to their equilibrium values with the emission of light at $6943\text{Å}$ (or possibly at somewhat longer wavelengths if intermediate transitions take place). In addition to the radiative transitions the upper state may be depleted by inelastic collisions with electrons, explaining the shorter decay time early in the afterglow. The giant scattering phenomenon seems more mysterious, and further investigation is needed; no doubt a substantial number of interesting laser-plasma interactions remain to be uncovered, and perhaps this will prove to be one of them.

## REFERENCES


IV-1. W. G. Wagner and B. A. Lengyel, J. Appl. Physics 34, 2040-46 (July 1963).

IV-2. G. Eckhardt, R. W. Hellwarth, F. J. McClung, S. E. Schwarz, D. Weiner, E. J. Woodbury; Phys. Rev. Letters 9, 455-57 (Dec. 1, 1962).

IV-3. A. V. Phelps and S. C. Brown, Phys. Rev. 86, 102-105 (1951).

IV-4. H. S. W. Massey, Negative Ions, Cambridge, (1950), pp.71-76.

IV-5. S. E. Schwarz, "Plasma Diagnosis By Means of Photon-Electron Scattering," Calif. Institute of Technology Quantum Electronics Laboratory Scientific Report No. 6, (Feb. 1, 1964).

IV-6. D. J. Rose, L. M. Lidsky and E. Thompson, 5th Annual Meeting of A.P.S. Division of Plasma Physics, San Diego, Calif. (Nov., 1963).

# APPENDIX A

## PHOTOMULTIPLIER RESPONSE CHARACTERISTICS

In the scattering experiments described in this thesis, the signal current leaving the photomultiplier detector is typically in the form of a pulse one to two milliamperes in magnitude, superimposed on a slowly varying background current of one to two milliamperes. To avoid errors resulting from non-linearity of the photomultiplier, the latter was wired in a manner designed to minimize such effects. Measurements were carried out on the phototube and its circuitry to determine what degree of non-linearity remained.

The photomultiplier tube was an EMI type 9558/B, having eleven dynode stages with, at the operating voltage of 1470 volts, an estimated current gain of $7 \cdot 10^5$. The wiring diagram is shown in Fig. A-1. The function of the capacitors is to stabilize the dynode voltages when current is drawn from them. One expects that as the photocathode is excited, electrons are lost from the dynodes, and, to the extent permitted by the capacitors, the dynodes become more positive, and the gain of the tube increases. In order to ascertain that this effect is not a source of error, a testing arrangement as shown in Fig. A-2 was used. Here the NE-2 lamp was used to produce a large current pulse through the tube. Then a short 0.2 microsecond pulse was produced by means of the Kerr cell, and the response to the second pulse as a function of the fatigue produced by the first pulse was noted. It was found that the percentage increase in sensitivity $\Delta$ was approximately

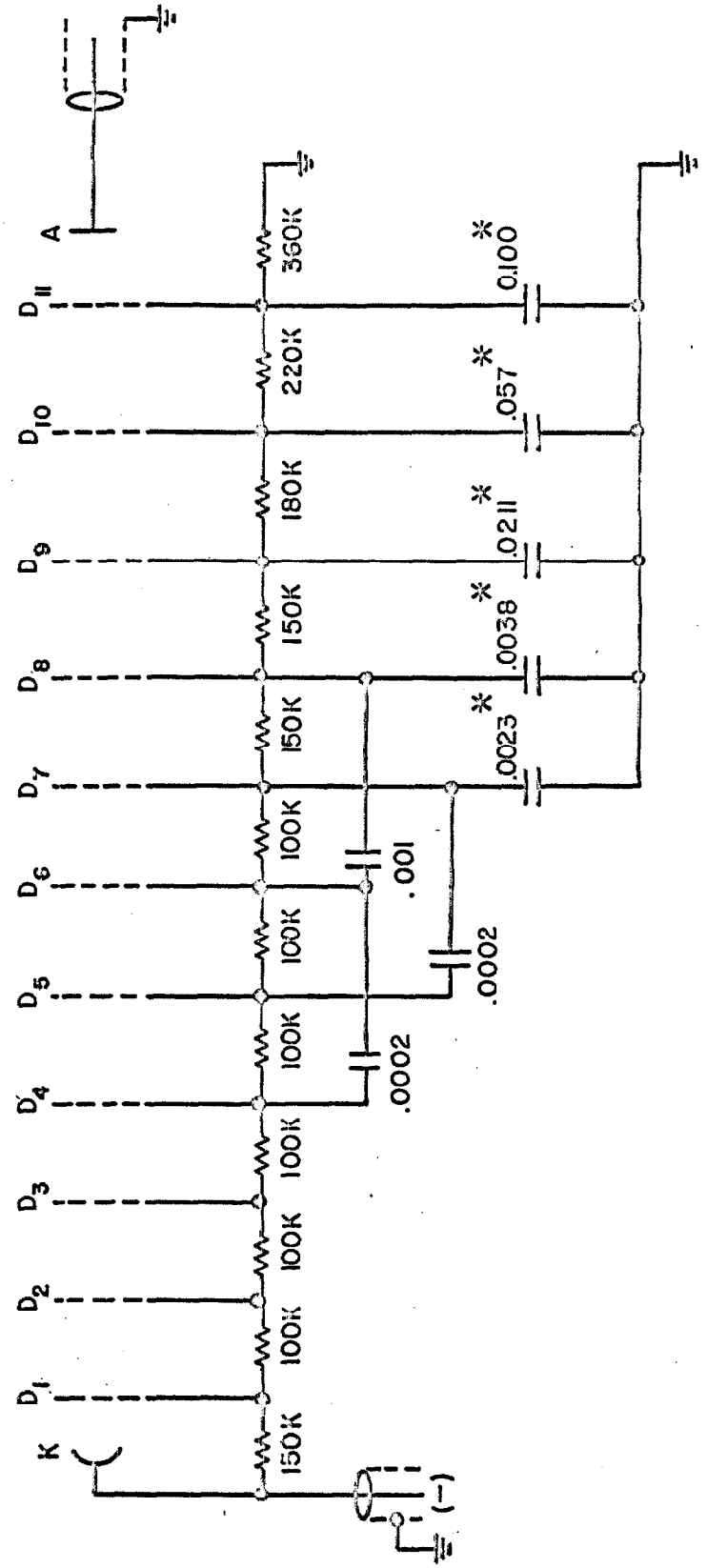


Figure A-1: Wiring diagram of 9558/B photomultiplier. Quantities with asterisks are measured values.

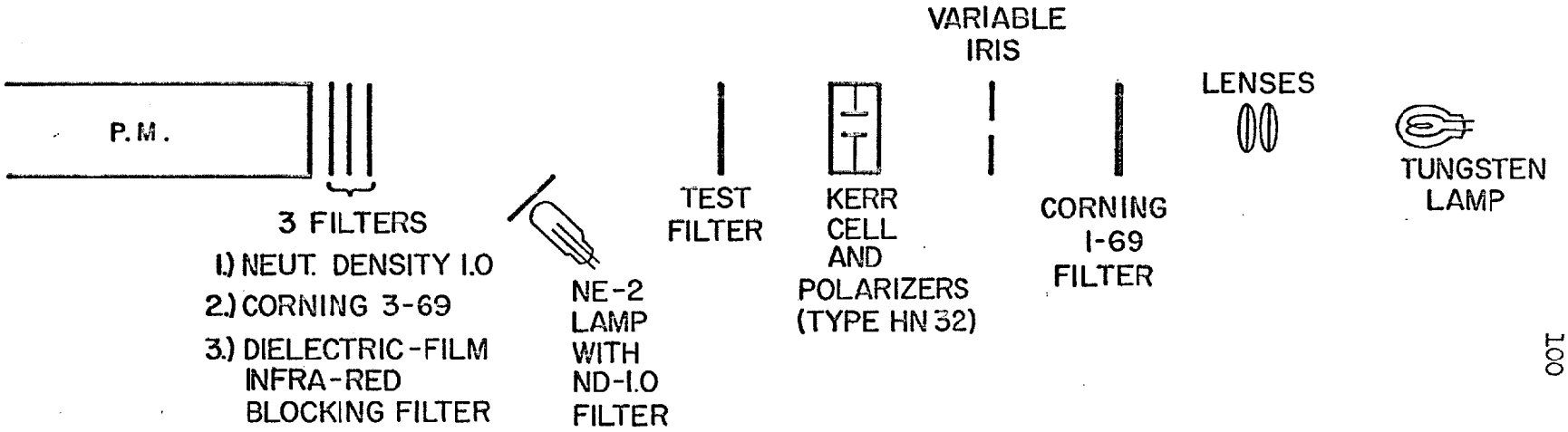


Figure A-2: Arrangement for photomultiplier linearity tests.

proportional to the charge previously taken from the anode, Q, according to the formula $\Delta = .0093Q$, where Q is in units of (microseconds) (milliamperes). This effect was therefore negligible in all of the actual experiments.

It was also necessary to determine the linearity of the tube at high peak currents. Referring again to Fig. A-2, the color filters were used to eliminate infrared radiation, confining the spectrum to the region of calibration of the neutral density filters. (These were found, by measurement at low current, to have their correct attenuation values.) The tube was then calibrated using 0.2 microsecond light pulses by means of test filters inserted as shown. The saturation curve obtained is shown in Fig. A-3. The dropping-off of gain is thought to be due to disturbance of the current flow by space charge. The corrections required for this effect, always small, have been made wherever necessary.

As a double check on the tube response an additional test was made, closely simulating the actual experiment. A slowly varying light pulse was produced by the neon lamp, and a short pulse of light through the Kerr cell injected on top of it. The magnitudes of the two pulses were noted separately, and note taken as to whether the response to the sum was related to the response to the parts according to Fig. A-3. Agreement was always found, within a few percent.

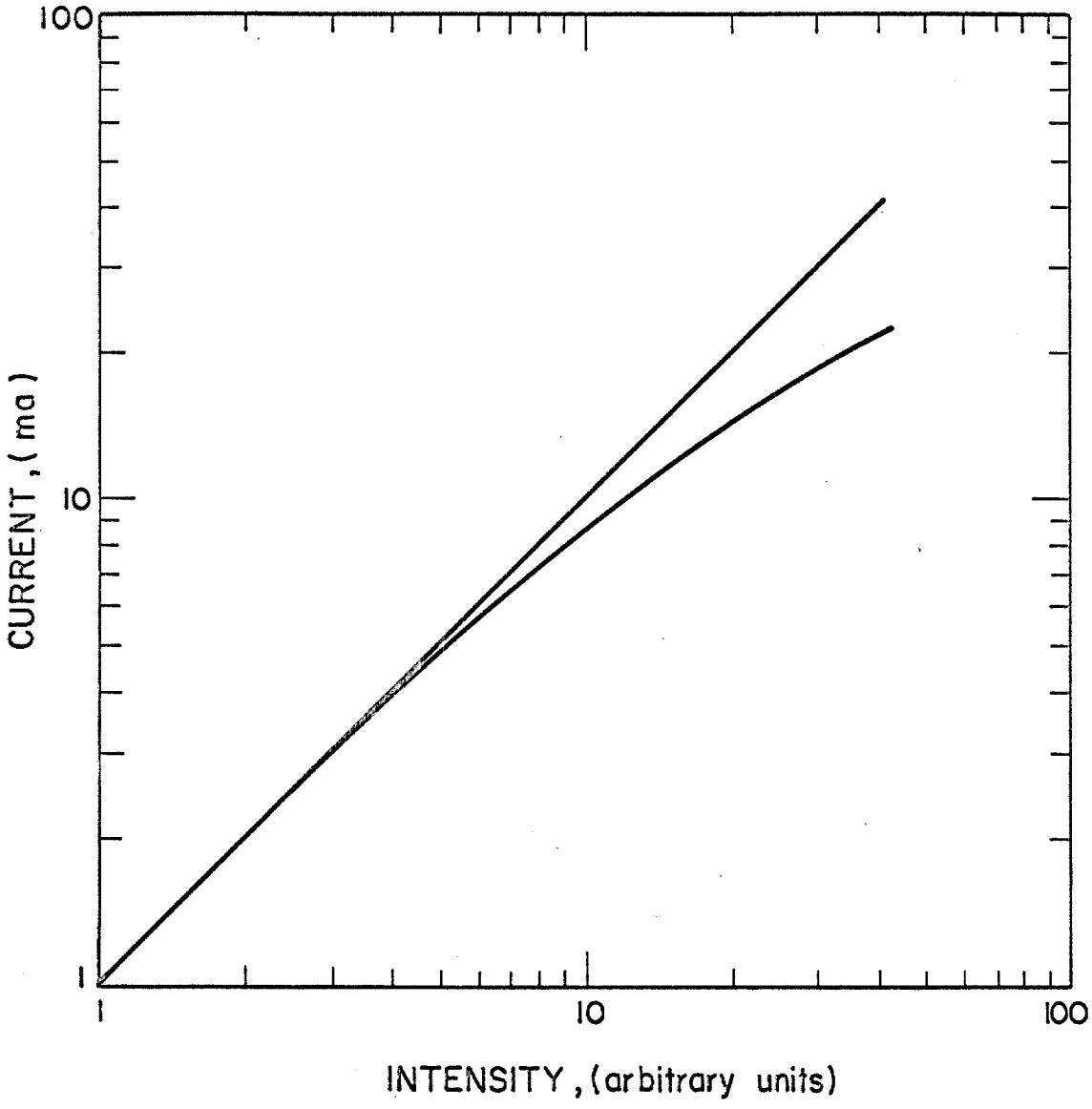


Figure A-3: Saturation behavior of 9558/B photomultiplier.
Upper curve is ideal linear response.
Lower curve is actual response.

# APPENDIX B

## THE GIANT-PULSE LASER

The giant-pulse laser was originally proposed by Hellwarth, [A-1] and was first constructed by McClung and Hellwarth.[A-2] Further studies of its properties have been carried out by McClung and Hellwarth [A-3] and by Wagner and Lengyel.[A-4] A diagram of the unit constructed for these experiments is shown in Fig. A-4.

The principle of operation is as follows. Initially the Kerr cell or Pockels cell (both were used) is raised to quarter-wave plate voltage, so that as light reflected from the righthand mirror traverses the cell twice, its polarization is rotated through $90^{\circ}$. The unwanted polarization is then rejected by the Wollaston prism. The manual trigger excites the flashlamp, which produces a population inversion between the $^{2}E$ excited state and the ground state of the ruby. The population cannot relax through laser action, because the feedback path via the righthand mirror is not available. After the inversion has reached its maximum (about 400 microseconds) the voltage is removed from the Kerr cell with a fall time of about .01 microsecond. Intense laser action then takes place and a "giant pulse" is produced.

The pulses emitted by this laser typically have peak powers in the range one to five megawatts, and duration (at half-power points) in the neighborhood of .03 microsecond. Oscillograph traces showing typical giant pulses are displayed in Chapter III.

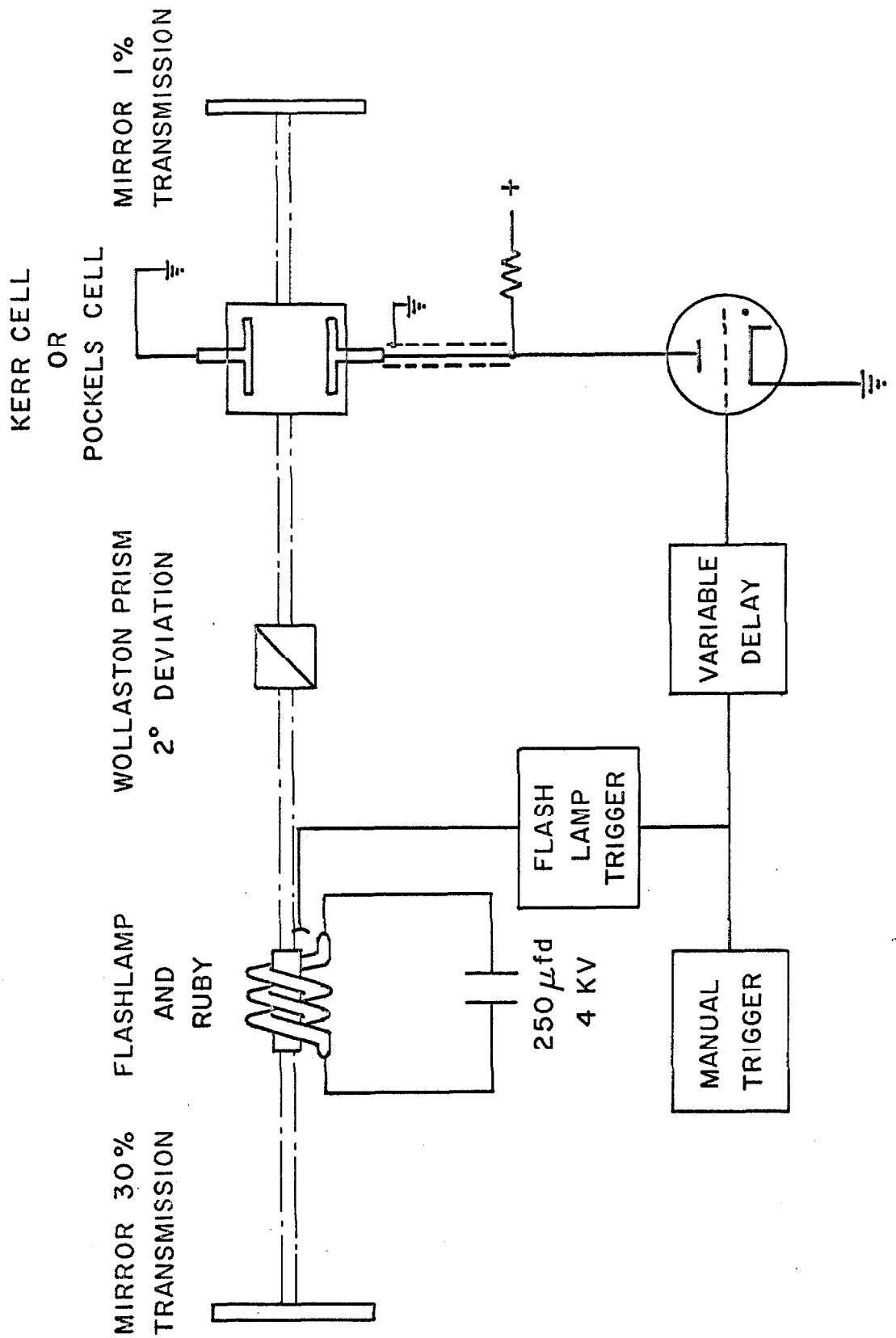


Figure A-4: Diagram of giant-pulse laser.

## REFERENCES

A-1. R. W. Hellwarth, Advances in Quantum Electronics, J. R. Singer, ed., Columbia University Press, 1961, pp.334-41.

A-2. F. J McClung and R. W. Hellwarth, J. Appl. Physics, 33, 828-31 (1962).

A-3. F. J. McClung and R. W. Hellwarth, Proc. I.R.E. 51, 46-53, (1963).

A-4. W. G. Wagner and B. A. Lengyel, J. Appl. Physics, 34, 2040-46 (July, 1963).